EXPERIMENTAL AND ANALYTICAL STUDY ON THE PERFORMANCE OF CEMENTITIOUS MIXES CONTAINING DIFFERENT RE-GENERATED END OF LIFE MATERIALS

A Thesis

by

Matineh Mahmoudi

Submitted to the

Graduate School of Sciences and Engineering
In Partial Fulfillment of the Requirements for
the Degree of

Master of Science

in the
Department of Civil Engineering

Özyeğin University
December 2022

EXPERIMENTAL AND ANALYTICAL STUDY ON THE PERFORMANCE OF CEMENTITIOUS MIXES CONTAINING DIFFERENT RE-GENERATED END OF LIFE MATERIALS

Approved by:

Assistant Professor. Dr. Zeynep Başaran Bundur, Advisor,
Department of Civil Engineering
Özyeğin University

Professor. Dr. S. Feyza Çinicioğlu,
Department of Civil Engineering
Özyeğin University

Professor. Dr. Mehmet Ali Gülgün,
Department of Metallurgy and Materials Science
Sabancı University

Date Approved: 20 December 2022

To my advisor, family, and friends

ABSTRACT

Cement, which is one of the main constituents of conventional concrete, is being manufactured every day around the world. because of the large demand for the material, the industry is responsible for 8% of the total global man-made CO_2 emission [1]. Thus, environmental considerations motivated researchers to find alternative replacements for cement in concrete that can reduce the harmful impacts of the concrete industry. Calcined clays are one group of Supplementary Cementitious Materials (SCMs); among them, metakaolin is the most reactive SCM recognized up to now [2]. However, due to its limited resources and uses in other industries, it has a relatively high price and it is not feasible to use it as a cement substitution in larger volumes. Therefore, treating and activating other potential materials in order to obtain an active cement replacement is the interest of many research projects nowadays.

Due to their high alumina and silica content, concrete demolition waste and mineral demolition deposit quarries can be suitable SCM candidates for cementitious systems. When these raw materials and End of Life (EOL) products (such as marble dust from quarries) are used directly, they are not chemically involved in the hydration processes needed for the setting and hardening of concrete and only act as a filler. However, appropriate mechanical and thermal activation procedures can destabilize the pozzolanic-active phases in EOL materials, might contribute to the hydration reactions, and replace a considerable portion of OPC. Nevertheless, there is a knowledge gap in experimentally activating the EOL materials and investigating their effects on cementitious systems when included at high percentages.

Thus, this study aims at understanding the performance of cementitious mixes containing regenerated EOL materials as SCMs up to 30% replacements. The influence of regenerated EOL materials was measured by fresh and hardened state tests, as well as durability assessments. The results showed that there was a general decrease in the workability and strength of EOL-containing samples, while the other results varied from one material to another. The experimental results were further used for generating analytical estimation models.

The outcomes of this study will enable utilization of EOL materials which would decrease the environmental problems of landfill accumulation. This will also create economic value for these large amounts of waste material that previously had zero value, as well as decreasing energy consumption, CO_2 emission, and the raw material costs of cement production. All of these factors contribute to the Horizon Europe targets in the European Energy Sustainability Initiative.

ÖZETÇE

Geleneksel beton üretiminin ana bileşenlerinden biri olan çimento, dünya çapında her gün milyonlarca ton üretilmektedir. Bu malzemeye olan büyük talep nedeniyle endüstrisi toplam küresel insan kaynaklı CO_2 emisyonunun %8'inden sorumludur [1]. Bunun sonucunda oluşan çevresel kaygılar araştırmacıları beton endüstrisinin zararlı etkilerini azaltabilecek betonda çimento yerine kullanılabilecek alternatif kaynaklar bulmaya yöneltmiştir. Metakaolin gibi kalsine killer beton üretiminde çimento ikamesi için sıklıkla kullanılmaktadır [2]. Bununla birlikte, özellikle kaolin kaynaklarının sınırlı olması ve sınırlı kaynakları diğer endüstrilerdeki kullanımı nedeniyle, metakaolinin diğer alternatif pozolanik malzemelere nispeten daha yüksek bir fiyata sahip olmasına neden olmaktadır. Bu da daha büyük hacimlerde çimento ikamesi olarak kullanılmasına bir engel oluşturmaktadır. Bu nedenle, metakaoline gibi doğal bir puzolanik malzemeye alternatif potansiyel malzemelerin işlenmesi ve etkinleştirilmesi günümüzde birçok çalışmanın araştırma sorusudur.

Yüksek alümina ve silika içerikleri nedeniyle, beton yıkım atıkları ve mineral yıkım depozit ocaklarından elde edilen atıklar metakaoline alternatif puzolanik malzemelerdirç Bu hammaddeler ve benzer Ömrünü Tamamlamış (ÖT) ürünler (taş ocaklarından elde edilen mermer tozu gibi) hiçbir işlem uygulanmadan doğrudan kullanıldığında, betonun priz alması ve sertleşmesi için gereken hidratasyon süreçlerine kimyasal olarak dahil olmazlar ve sadece dolgu maddesi olarak işlev görürler. Ancak, uygun mekanik ve termal aktivasyon prosedürleri ÖT malzemelerindeki puzolanik-aktif fazları aktive edebilir, hidratasyon reaksiyonlarına katkıda bulunabilir ve karışımda çimentonun önemli bir kısmının ikame edebilir. Bununla birlikte, ÖT malzemelerinin

deneysel olarak etkinleştirilmesi ve yüksek oranlarda dahil edildiklerinde çimentolu sistemler üzerindeki etkilerinin araştırılması konusunda bir bilgi boşluğu bulunmaktadır.

Bu çalışma, çimento miktarının bir kısmı rejenere edilmiş ÖT malzemeler ile ikame edilen içeren çimentolu karışımların performansını anlamayı değerlendirmeyi amaçlamaktadır. Rejenere ÖT malzemelerinin etkisi, taze ve sertleşmiş durum testlerinin yanı sıra dayanıklılık değerlendirmeleri ile ölçülmüştür. Sonuçlar, ÖT içeren numunelerin işlenebilirliğinde ve dayanımında genel bir düşüş olduğunu, diğer sonuçların ise malzemeden malzemeye değiştiğini göstermiştir.

Bu çalışmanın sonuçları, ÖT malzemelerinin çimento ikamesi olarak kullanımını mümkün kılacak ve atık depolama sahalarında biriken çevresel sorunları azaltacaktır. Bu aynı zamanda, daha önce sıfır değere sahip olan bu büyük miktardaki atık malzeme için ekonomik değer yaratacak ve enerji tüketimini, CO_2 emisyonunu ve çimento üretiminin hammadde maliyetlerini azaltacaktır. Tüm bu faktörler, Avrupa Enerji Sürdürülebilirliği Girişimi'ndeki Horizon Europe hedeflerine katkıda bulunmaktadır.

ACKNOWLEDGMENTS

First of all, I would like to thank my advisor, Asst. Prof. Dr. Zeynep Başaran Bundur, for her unconditional support during my M.Sc. program. Passionate about research, professional in work, serious about science, considerate of my creative ideas, outstanding instructor, kind and caring, or briefly, the best advisor I could ever imagine. Being supervised by her and being a member of her research group was a miracle in my life.

I cordially acknowledge my committee my committee members; Prof. Dr. Feyza Çinicioğlu and Prof. Dr. Mehmet Ali Gülgün for contributing and supporting my thesis. This thesis was completed with financial assistance from the Scientific and Technical Research Council (TÜBİTAK) of Turkey (Project Title: Recement/ Project No: 119M840)

I would like to thank all of my lab mates for their help and the things I learned from them, especially Ilgın Sandalcı. My laboratory work relied on her so much and I could not have accomplished my work without her help.

I would like to thank my other instructors during my M.Sc. program for teaching me part of their knowledge and kindly answering my questions and educational demands during these four semesters. Thanks to Prof. S. Feyza Çinicioğlu, Dr. Taner Yılmaz, Dr. Hande Özturk, Dr. Senem Seyis, and Dr. Bekir O. Bartın. In addition, I would like to thank Ms. Gizem Bakır and Ms. Gizem Tekin Akbaş from graduate students' office for all her help and guidance.

I would like thank Prof. Mehmet Ali Gülgün and Dr. Mirijam Vrabec, two of the

leaders of our ERA-MIN2 project, on which I have based my thesis, and Yasemin Akyol, from Sabancı University, for all their help and efforts throughout the project.

I would like to thank my parents. My whole life they have stood like a barrier to all of problems and provided the best of everything so I can comfortably live and follow my goals. They have tolerated the hardship of me being away for education during these years, and still have supported me with my choices and believed in me.

I would like to thank my friends in Iran, Turkey, and Canada because of all of the help and support they have sent to me. They have always been kind to me while they did not have to be, and this is exceedingly precious.

Finally, in these days, I would like to mention the names of martyrs of freedom, women and men who are fighting and standing with each other, for my country Iran and for a better world.

TABLE OF CONTENTS

LIST OF TABLES

LIST OF FIGURES

NOMENCULTURE

ABBREVIATION	DEFINITION
MK	Metakaolin
RM	Red mud
IZ	Construction Debris from Izola
MB	Construction Debris from Maribor
SG	Construction Debris from Slovenj Gradec
NM	Construction Debris from Novo Mesto
CH	Portlandite, $Ca(OH)_2$
C-S-H	Calcium Silicate Hydrate
SP	Superplasticizer
OPC	Ordinary Portland Cement
CAC	Calcium Aluminate Cement
SCM	Supplementary Cementitious Materials
EOL	End of Life
ANN	Artificial Neural Network
ASR	Alkali Silica Reaction
DI	Distilled
RMSE	Root-mean-square error
s	Second
hr	Hour
min	Minute

MPa	Mega Pascal
g	Grams
kg	Kilograms
cm	Centimetres
M	Molar
ml	Millilitres
m^2	Square meter
kN	Kilonewton
°C	Celsius degrees

CHAPTER I

INTRODUCTION

Partial replacement of Ordinary Portland Cement (OPC) by Supplementary Cementitious materials (SCMs) has been the subject of several research due to concerns over the CO_2 emissions from OPC production. Some of the known SCMs are Fly ash, Slag, Silica fume, and Metakaolin (MK). These materials have shown successful performance in concrete when partially replaced the cement content. However, their low availability and their uses in other industries influence the feasibility of using these materials as SCMs in large volume in the concrete industry. Thus, the question of finding new and more widely available SCMs still remains. These SCMs would decrease the need for OPC in concrete, and in turn, would reduce the demand for the production of cement. Another group of potential SCMs is End of Life (EOL) materials, which can be a possible answer to the above-mentioned research problem. In previous studies, EOL materials, such as marble dust from quarries, have been used in concrete mixes as fillers. These materials, when applied directly and without treatment, do not contribute to the hydration process needed in concrete for setting and hardening.

Yet, the EOL materials are not only limited to the marble dust, the list can also be extensive. Herein, recent studies showed that construction demolish waste (CDW) and mine tailings can possess pozzolanic activity. As so, these materials are being used in geopolymer mixes which require pozzolanic behavior. Several articles have investigated CDWs and tailings from gold, phosphate, iron ore, and other mines as

precursors in geopolymer concrete, and have shown successful results [3]–[6]. It has been reported that the reactivity of these materials depends on their chemical phase composition and the initial mechanical/thermal treatment performed on them [7]. However, there is need for more studies on the fresh and hardened states of these mixes, as well as their durability [4].

Although geopolymer concrete has high strength and durability, but the difficulty and sensitiveness of the production process decreases the robustness of using geopolymer concrete in large volumes. Thus, using the EOL materials in conventional concrete as an SCM is a promising idea. Effectively regenerated EOL materials can support hydration processes and take the place of a significant amount of OPC. Nevertheless, the suitable activation process and properties of the mix containing those EOL materials remain unknown.

Thus, the main goal of this study is understanding the performance of cementitious systems containing high percentages of regenerated EOL materials. The specific research objectives followed in this study in order to accomplish the aforementioned aim are:

1. Using recycled SCMs as binding agents by mining and regenerating them: Collecting and analyzing the chemical and physical characteristics of EOL materials useable as SCMs in cement-based materials that are mined from construction, ceramic, and quarry sites. Choosing the mechanical and/or thermal treatments that reactivates the EOL materials. Examination of the pozzolanic (or hydraulic) behavior of SCMs that have been regenerate.

2. Assessing performance of cement-based materials, including SCMs that have been regenerated: Examining the effects of substituting regenerated SCMs for OPC (up to weight percentage of 30%) on the cement-based mix in terms of setting, workability,

rheology, compressive strength, water absorption, and chemical composition. Then, preparing estimation models for predicting compressive strength based on mix design and curing condition.

3. Assessing concrete's durability with regenerated SCMs: Examining the resistance of SCM containing mixes to sulfate attack and alkali silicate reaction (ASR). Finding the connections between the pozzolanicity of EOL materials, their mineralogy and sources, and their replacement percentages in the concrete mix with the performance and lifespan of the concrete mixes containing those materials.

All of the above-mentioned methods are presented in the methodology chapter, and the results are discussed in the results and discussion chapter, as well as a conclusion in the final stage.

The broader impact of outcomes of this study are all in alignment with Horizon Europe targets in the European Energy Sustainability Initiative, which is crucial due to environmental concerns in today's world. A number of these outcomes are:

1. Actualizing regeneration and usage of EOL materials slated for landfill as a raw material for concrete production; giving economic value to huge amounts of material that have previously had zero value while lowering energy consumption, CO_2 emissions, and costs of cement production.

2. Making improvements in sustainable construction materials area by decreasing raw material consumption and greenhouse gas emissions from cement production.

3. Engaging the norms of recycling and reusing EOL materials in the concrete industry.

These are all in alignment with Horizon Europe targets in the European Energy Sustainability Initiative, which is crucial due to environmental concerns in today's

world.

CHAPTER II

LITERATURE REVIEW

2.1 Conventional concrete, advantages and disadvantages

Concrete is the most used building material in today's world [8]. Concrete has several advantages as a building material. Since concrete is a viscous material before hardening, it can be formed with favorable moulding into various geometrical shapes. The material used in concrete is available everywhere around the world. In comparison with steel structures that collapse when subjected to fire, concrete shows good fire resistance. Unlike high corrosion and oxidation of steel and possibility of erosion and decomposition of wood, concrete shows good resistance in various environments and does not have huge maintenance costs. However, concrete industry has high CO_2 emission, and the production process consumes large amounts of energy.

Ordinary Portland Cement (OPC) is the most common binder used in concrete. This common cement is a hydraulic binder, meaning that the hardening process and bonding formation happens in presence of water. The biggest problem of the conventional cement is the high CO_2 generation during manufacturing process. In this manufacturing process first the raw material which contains limestone (calcium carbonate) and some other silicates and oxides such as silicon dioxide, aluminum oxide, and ferric oxide are grinded and then heated up to almost 1450℃. During the heating the following reactions take place:

$CaCO_3 \rightarrow CaO + CO_2$

During this reaction the CO_2 is emitted and CaO is consumed as follows:

$2CaO + SiO_2 \rightarrow 2CaO \cdot SiO_2$ (Alite) (Also written as C_2S)

$3CaO + SiO_2 \rightarrow 3CaO \cdot SiO_2$ (Belite) (Also written as C_3S)

$3CaO + Al_2O_3 \rightarrow 3CaO \cdot Al_2O_3$ (Tricalcium aluminate) (Also written as C_3A)

$4CaO + Al_2O_3 + Fe_2O3 \rightarrow 4CaO \cdot Al_2O_3 \cdot Fe_2O_3$ (Brownmillerite) (Also written as C_4AF)

These resulting compounds which form the "clinker" are then powdered and mixed with gypsum and the cement production process is then finished. Thus, there are two agents of CO_2 generation in cement manufacturing:

1. The emitted CO_2 in the first chemical reaction (60% of the total CO_2 emission); and

2. The emitted CO_2 of burning fossil fuels in order to provide the heat needed for clinker formation (40% of the total CO_2 emission). Each ton of cement production emits approximately 0.9 ton CO_2 [9]. Also, because of high demands of concrete and around the world, the overall cement production is higher than 4 billion tones each year, which is responsible for more than 5% of the total CO_2 production by humans' activities around the globe [9]. Also, it is important to mention that the energy used to produce this amount of cement is 10-11 EJ which is around 2-3% of the primary energy used in the world [9].

2.2 Supplementary Cementitious Materials (SCMs)

Researchers have been trying to find other substituents for ordinary cement with lower CO_2 emission and less energy usage in the manufacturing process. These materials contribute to the strength gain of concrete with hydraulic, pozzolanic, or partial hydraulic and partial pozzolanic activity. In the hydraulic reaction, alite and

belite phases react with water forming C-S-H (tobermorite) and CH (portlandite) phases. The main phase contributing to binding effect of the cement or SCMs is C-S-H phase. On the other hand, Pozzolans are siliceous or siliceous and aluminous materials that possess little cementitious value by themselves. However, if they are finely divided in the presence of moisture, they will react with calcium hydroxide CH to form calcium silicate hydrate (C-S-H) and other cementitious compounds. With increase of the C-S-H gel, the strength of concrete increases. Thus, if pozzolans are used, more C-S-H is produced with same amount of cement. Or, it would be possible to gain specific strengths with less cement usage. Also, reduction of CH improves the durability of cement paste by making the paste dense and impervious. Some of these binders are introduced briefly in this section:

Silica fume: Is a byproduct in production process of silicon and/or ferrosilicon alloys. This material is collected from the gas outlet of the related factories by means of filters. This is done to prevent entrance of this material into the environment and causing air pollution. Silica fume is authenticated as a pozzolan since 1987 [10]. It is found that when substituting cement with silica fume between 15% to 20%, the Elastic modulus, toughness, and steel-concrete bond can be improved.

Slag: Is a byproduct in manufacturing process of steel. It is found that when the slag is water-quenched during the production process, it gains hydraulic/pozzolanic characteristics and can be used as partial binder in concrete. Slag makes concrete more durable and gives higher long-term compressive and flexural strength [11].

Fly ash: Is a byproduct in electricity generation power plant, when coal is burned. Fly ash is also collected from the gas outlet of the power plant by means of filters. When fly ash is used, the concrete becomes more workable, can gain higher

strengths, and several other benefits [12].

Calcined clay: Is produced by treating clays under certain condition which gives them pozzolanic characteristic [13]. Metakaolin or calcined kaolinite has shown great pozzolanicity compared to other calcined SCMs since kaolinite is a 1:1 clay with high percentage of Si phases [14], [15]. Some of the other clays studied for calcination and using as SCMs are namely illite, montmorillonite, bentonite, zeolite, and sepiolite [16]–[19].

EOL materials: Some of the previously studied EOL materials are agricultural remnants, ceramic debris, and glass rejects which have shown promising results when used as SCMs or as precursors in geopolymer concrete [20]–[22].

2.3 End of Life materials as SCMs

These named SCMs although have shown promising results when used in concrete mixes but their amount being produced is far behind the demand for concrete in the world. Since they are mostly by products of other industries and their production is limited by the main industry. Their usage in other industries and regional availability are other reasons that makes their usage in concrete non-feasible. However, there is another group of EOL materials which is from urban quarries. These widely available materials can be low energy alternative binders, since regenerating them into SCM lowers the costs and energy consumption, at both production and transportation stages. Recycled EOL materials from quarries have been mostly used as aggregates or fillers [23]. However, the most energy consuming constituent of concrete is cement. Thus, recycling cement from concrete remnants, which normally goes to landfills after demolition, would be of greater benefit. The cement existing in these debris is previously hydrated and consists of calcium silicates/aluminosilicates and calcia phases.

These phases can be regenerated into SCMs with heat and/or mechanical treatment. In fact, construction debris are not the only EOL materials containing these regeneratable phases. Remnants of the ceramic industry, marble and copper mining also contain significant amounts of silicates/aluminosilicates and calcia phases [24]. However, these sources also have been mostly used as fillers or aggregates [25], [26]. However, it has been recently discovered that construction demolish waste (CDW) and mine tailings can have pozzolanic activity. Thereafter, these materials have been used in geopolymer concrete where pozzolanic behavior is required. Some of the studied CDWs and tailings are from gold, phosphate, iron ore, and other mines, and they have shown promising results [3]–[6]. However, although geopolymer mixes have higher strength and durability, they are difficult to produce of and are sensitive to production process which would decreases the feasibility of their application. Thus, using the EOL materials in conventional concrete as an SCM would be of greater benefit.

The thermal and mechanical energy needed for reactivating these phases is considerably less, compared to OPC production [27], [28]. Besides, these materials with high regeneration potentials have zero value now and are being deposited in nature. Thus, giving economic materials to them and stopping their accumulation on earth are other benefits of using these EOL materials as SCMs. This idea can reduce the CO_2 emissions by 15% per kg of OPC regarding the raw material replacement, and 56% reduction in power consumption for binder production.

Since the types and percentages of the named phases vary in different EOL materials, it is of great importance to determine the characteristics of them and the performance of the mixes containing them. These properties affect the activation temperature, mechanical griding, as well as optimized percentage of cement

replacement.

CHAPTER III

MATERIALS AND METHODS

3.1 Material Selection and Mix Design

In the conventional mortar system, the main constituents are sand, water, binder, and optional admixtures. In this study, mortar samples were prepared with cement replacement percentages of 15%, 20%, 25%, and 30%. The control samples were prepared so that the SCM-containing samples can be compared with them and the effect of SCM on the properties of the mix can be understood. The binder in the control samples was 100% Portland cement (CEM I 42.5R). Besides, since all of the SCM-containing samples needed a superplasticizer (SP) to have proper workability, two sets of negative control samples were produced: one with SP and one without it. The SP content in cement paste samples were kept constant at 0.5% by weight of the binder. The amount of SP in all of the mortar mixes is adjusted such that the flow table results (see sections 3.3 and 4.1) of the mix remains within ±15% difference with the negative control sample containing SP (Control_SP). A superplasticizer (SP) based on polycarboxylic ether (PCE) polymers (BASF) and EN 196-1 standard sand was used in this study [29]. The mix design of mortar and paste samples are presented in Tables 1 to 3. The water to binder ratio was 1 to 2 and sand to binder ratio was 3 to 1 for all tests.

Table 1: Mix design data of MK containing samples

Sample names		*Cement (g)*	*MK (g)*	*Water (g)*	*Sand (g)*	*SP (g)*
Control	Control	450	0	225	1350	0
	Control_SP	450	0	225	1350	1.12
Metakaolin	MK_15	382.5	67.5	225	1350	4.5
	MK_20	360	90	225	1350	4.5
	MK_25	337.5	112.5	225	1350	6
	MK_30	315	135	225	1350	9

Table 2: Mix design data of RM containing samples

Sample names		*Cement (g)*	*RM (g)*	*Water (g)*	*Sand (g)*	*SP (g)*
Control	Control	450	0	225	1350	0
	Control_SP	450	0	225	1350	2.25
Red mud	RM_15	382.5	67.5	225	1350	4.5
	RM_20	360	90	225	1350	4.5
	RM_25	337.5	112.5	225	1350	6
	RM_30	315	135	225	1350	9

Table 3: Mix design data of IZ containing samples

Sample names		*Cement (g)*	*SCM (g)*	*Water (g)*	*Sand (g)*	*SP (g)*
Control	Control	450	0	225	1350	0
	Control_SP	450	0	225	1350	1.12
Izola	IZ_15	382.5	67.5	225	1350	1.12
	IZ_20	360	90	225	1350	2.25
	IZ_25	337.5	112.5	225	1350	2.25
	IZ_30	315	135	225	1350	2.25
Maribor	MB_15	382.5	67.5	225	1350	2.25
	MB_20	360	90	225	1350	2.25
	MB_25	337.5	112.5	225	1350	2.25
	MB_30	315	135	225	1350	2.25
Novo mesto	NM_15	382.5	67.5	225	1350	1.12
	NM_20	360	90	225	1350	1.12
	NM_25	337.5	112.5	225	1350	1.12
	NM_30	315	135	225	1350	1.12
Slovenj Gradec	SG_15	382.5	67.5	225	1350	1.12
	SG_20	360	90	225	1350	1.12
	SG_25	337.5	112.5	225	1350	1.12
	SG_30	315	135	225	1350	1.12

Three different types of SCMs were tested in this study. The first SCM is commercial Metakaolin (MK). Samples containing MK were prepared in order to have the upper limit of the performance of SCM-containing mixes, since MK is the best-known calcined SCM up to date. The next SCM was Red mud (RM). This EOL material was initially obtained from the residues of bauxite rock in the aluminum industry and treated before being included in the mortar mixes. RM was ground and heated up to 850 °C for treatment. The most prominent phases present in the calcined RM were Mayenite and Hematite, which consist of iron, aluminum, and calcium oxides. The third group of SCMs were the construction debris from 4 different locations, namely Slovenj Gradec (SG), Maribor (MB), Izola (IZ), and Novo mesto (NM). These were also EOL materials that were separated from urban queries and mechanically and thermally treated. These materals were also ground and heated up to 1100 °C. The prominent phases in these materials were Calcite, Dolomite, Quartz, and amorphous content. The particle size distribution of these samples is presented in Table 4. More detailed characteristics of the used materials can be found in Appendix A.

Table 4: Particle size analysis of materials

Material names	D_{10} (μm)	D_{50} (μm)	D_{90} (μm)
OPC	4.27	13.8	34.0
MK	2.38	7.28	21.9
RM	3.96	34.1	132
IZ	15.5	127	248
MB	2.17	7.38	25.9
NM	3.54	46.9	112
SG	2.20	6.68	29.5

3.2 Mixing Procedure of Mortar and Paste

The mixes were prepared based on ASTM C305-14 standard for both mortars and pastes [30]. First, the dry binder content (cement and SCM) was mixed for 30 s on slow mode (62 rpm). The SP content was added to the mix water. Then, the SP-water mixture was added to the blended dry binder. The cement paste mix was mixed at slow speed for 30s. For cement paste samples, the mix was manually scraped for 15 s at this stage. At the final step, the paste was mixed on fast mode (125 rpm) for 60 sec. For mortar samples, the sand was added after mixing binders with water, and mixing was continued first on 30 s slow and 30 s on fast mode. The mix was manually scraped and rested for 45 s at this stage. Finally, the mortar was mixed for another 60 s on fast mode.

3.3 Fresh State Performance Assessment

3.4.1. Workability- Flow table

In order to understand the workability of mortar mixes, a simple flow table test was performed according to ASTM C1437-15 [31]. In this test, the cone is filled in two steps and compacted with the hammer by 20 releases at each step. The surface is then scraped to remove the excess mix and the cone is pulled up. Then, the table was raised and released once a second for 25 times. The diameter of the mix on the table was measured on 4 angled lines (diameters) and averaged. The test was repeated for three mixes and the average value is reported as a result. .

3.4.2. *Initial Setting Time*

The initial setting time of binder pastes was determined by the Vicat needle test. For this test, the paste was placed into the special molds, and if needed, the mold was gently tapped to a table for compaction, ensuring no segregation. The needle was fixed close to the surface of the mold and released every 15 mins until the first signs of setting were observed. The releasing repentance was then increased to once a 5 mins. The initial setting time was considered the time when needle penetration inside the paste was 2.5 cm.

3.4.3. *Workability- Rheology of cement paste*

For determining the rheological properties of the binder pastes, a commercial rotational rheometer (Anton Paar Rheolab QC) was used with a vane and a container (Figure 1). The flow curves were derived using a controlled shear rate flow curve (CSR) test protocol. In this test, the pastes were placed inside the rheometer container immediately after mixing and sheared for 60 s at 300 s^{-1} for the pre-shearing stage. This stage is done so for eliminating the effects of shear stresses applied to the paste during mixing as well as the agglomeration of binder particles [32]. The paste was then kept at rest for five minutes to be stabilized after high-rate pre-shearing. For obtaining the flow

curves, the shear rate was first increased from 0 to 100 s^{-1} in 60 s to obtain the up-curve, and then decreased from 100 to 0 s^{-1} again in 60 s to obtain the down-curve. The rheological properties of plastic viscosity and dynamic shear stress were extracted from the resulting down-curve by fitting the Bingham's equation to them (Equation 1):

$$\tau = \tau_0 + \mu\gamma \quad (1)$$

Where τ_0 is the dynamic shear strength [Pa], μ indicates the viscosity [Pa.s], and γ represents the shear rate [s^{-1}]. Bingham's model is the most frequently used model for determining the rheological properties of cementitious mixes.

.

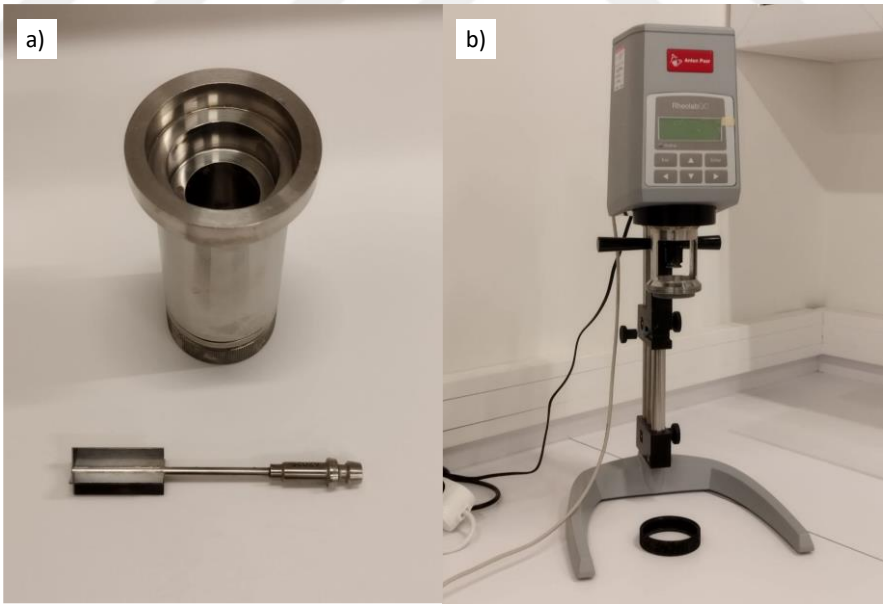

Figure 1: Rheology test set up: a) Vane and container, and b) Rheometer

3.4 Compressive strength

To measure the compressive strength of mortar samples, first series of 5*5*5 cm cubes were cast according to ASTM C109/C109M-20 [33]. The molds were filled with fresh mix in two stages and rodded and compacted after each stage. After scraping the surface, the molds were kept in humid environment at 21 °C for 24 hr. Then, the samples were demolded and cured in a humidity chamber at 22°C with RH>95% until the test dates. The cured cubes were tested at 3, 7, 28, and 90 days in accordance with NBN EN 196-1 [29]. The compressive strength was determined by using a 2000 kN servo hydraulic load-controlled device. The loading rate was kept at 2 kN/s. The test was with triplicates of samples and the average value is reported as a result.

3.5 Compressive strength estimation method using multiple linear regression

Linear regression equations were derived based on the experimental compressive strength results. In these equations, the compressive strength of samples was related to the percentage of cement replaced with one of the SCMs, the percentage of SP to binder ratio, and the age of samples. For each SCM, a matrix of values of the changing variables is formed, as well as the vector of corresponding strength values. Since the model is assumed to be linear, the matrix and the strength vector can be related together with a series of coefficient [34]. The parametrical equation is shown in Equation 2 and 3:

$$\begin{Bmatrix} y_1 \\ y_2 \\ \vdots \\ y_n \end{Bmatrix} = \begin{Bmatrix} 1 & x_{11} & x_{12} & \dots & x_{1m} \\ 1 & x_{21} & x_{22} & \dots & x_{2m} \\ \vdots & \vdots & \vdots & \dots & \vdots \\ 1 & x_{n1} & x_{n2} & \dots & x_{nm} \end{Bmatrix} \begin{Bmatrix} b_0 \\ b_1 \\ b_2 \\ \vdots \\ b_m \end{Bmatrix} + \text{error} \quad (2)$$

$$y = b_0 + b_1 x_1 + b_2 x_2 + \cdots \quad (3)$$

Where "n" is the number of observations and in each of them there are "m" variables that will have the same coefficient values for all observations with differing values. After calculating the vector of coefficients, the regression equation for compressive strength is derived as the summation of multiplication of each coefficient and the corresponding variable. In this study, there are three changing parameters of SCM percentage, SP to binder ratio percentage, and curing days. Therefore, the final equation form is shown in Equation 4:

$$y = b_0 + b_1 * (\%SCM) + b_2 * \left(\% \frac{SP}{binder}\right) + b_3 * (age(days)) \quad (4)$$

The coefficient of determination or R^2 is also calculated for understanding the accuracy of the final equation.

3.6 Compressive strength estimation method using Artificial Neural Network (ANN) technic

An ANN model was generated based on the experimental results of the compressive strength test. Similar to the regression method, the input variables chosen for generating the model were the percentage of cement replaced by SCM, the

percentage of SP to the binder, and days of curing. In an ANN model, the inputs are given to the units of the input layer and the desired output is obtained from the output layer. The output result of the model used in this study is a single value of compressive strength. In the middle, there are one or more parallel hidden layers that transform the information. Each hidden layer consists of a number of neurons, and all neurons of two successive layers are interconnected with weights. The number of hidden layers and the number of neurons in the hidden layers were chosen by trial and error. The learning method used in this study is defined as the comparison of the compressive strength and estimated values, and the error is given back to the model. The weights of the model are then adjusted based on the errors. During a number of epochs, the error of the model is minimized.

Each input value was given to the model as the weighted sum of those values. The parametric output of the first hidden layer given to the second layer is shown in Equation 5:

$$y_{pj} = \sum_{i=1}^{n} w_{ij}\, a_{pi} + b_{pj} \tag{5}$$

Where b_{pj} is the bias for j^{th} neuron in the first hidden layer, a_{pi} is each output of the first layer sent to the second layer, w_{ij} is the weight value between each neuron in the input layer and each neuron in the first hidden layer, and n is the number of inputs sent to the first hidden layer. Then, for normalizing the outputs of hidden layers, sigmoid function is applied (Equation 6):

$$\sigma(y) = \frac{1}{1 + e^{-y}} \tag{6}$$

When the training is finished, the results are validated using another set of data.

3.7 Water absorption

The water absorption of samples was measured following the RILEM 25 PEM II-6 test standard [35]. Three mortar cubes of each mix design were used for this test. The samples were first cured for 28 days in a similar condition with compressive strength cubes. After that they were placed in an oven at 40 °C and periodically weighed until their weight change maintained within ±0.1% range, which indicated that the water inside voids and capillary pores had evaporated. Then, four sides of the cubes were covered with epoxy to waterproof them, leaving two facing sides uncoated to absorb water and to restrict water flow direction. The weight of dry cubes was measured at this stage (W_0), and then they were placed in a water tank such that the water surface was 25 mm higher than the surface of the cubes. The uncoated faces of the cubes were facing up and down. Besides, holders were used in order for the cubes not to touch any surface of the container. The weight of the cubes was measured repeatedly at 15 and 30 minutes and 1, 2, 3, 8, 12, 24, 48, 72, 96, and 120 hrs after being submerged in water (W_w). Before each weighting, the cubes were gently wiped to remove excess surface water. The water absorption coefficient (k) was derived from Equation 7:

$$k = \frac{Q}{A\sqrt{t}} \tag{7}$$

Where “Q” is the net mass of absorbed water (W_w – W_0) in [kg], “A” is the uncoated surface area of the cube in [m^2], and “t” is the time spent submerged in [s].

3.8 Sulfate attack

Sulfate attack test was done by using 5*5*20 cm length changing beams. The sulfate attack test is done according to the ASTM C1012/C1012M-18b standard [36]. For this test, a control sample without superplasticizer was not produced because of low workability. Also, for SCM-containing samples, only samples with 25% cement replacement were prepared. Three samples of each mix design were prepared. For this test, beams were cast and placed in sealed container on raisers, and the container was filled with 35±3°C water such that the water did not exceed the top of the risers. The samples were kept in the container with constant temperature of 35±3°C for 1 day. Then, they were demolded and placed in the humidity chamber with RH>95% and 23.0±2.0°C condition. To make sure that the samples had 20MPa compressive strength before starting the test, they were kept for another two days in the chamber, according to our results from section 3.4. The sulfate solutions were prepared one day before immersion, such that first 50 g of anhydrous sodium sulfate (Na_2SO_4) was added to 900 ml of DI water and then the solution was further diluted until the volume of solution reached to 1 liter. After curing, the length of samples was measured using the length change comparator and then they were placed in the solutions. The volumetric ratio of solution to sample was kept at 3.5. Periodic length measurements were done at 1, 2, 3, 4, 8, 13, 26, and 39 weeks. After each measurement the solution was renewed, and the samples were placed into a fresh solution.

3.9 Alkali silica reaction (ASR)

For the ASR test, the mix designs used, and casting procedure were same as the sulfate attack test (section 3.8). This test was performed based on ASTM C1567-21 standard [37]. The samples were cast, covered with wet towel, and cured at 23°C in humidity chamber for 24 hr. Then, after demolding, their length was measured using comparator and then they were immersed in 23.0±2.0°C tap water. After that the container was sealed and placed in oven at 80.0±2.0°C. Meanwhile, the solution was prepared by adding 50 g of anhydrous sodium hydroxide (NaOH) to 900 ml of DI water and diluting it until 1 liter of solution is obtained. The ratio of volume of solution to the volume of sample was kept at 3.5. After 24 hrs, the samples were removed from the water curing and the length was measured. Then, they were transferred into the NaOH solution at 80.0±2.0 °C. According to the standard, at least three readings must have been done during the first two weeks after immersion. In this case, the lengths were measured at 4, 8, and 12th day. Then, for understanding long term exposure effects, the samples were measured at 160, 180, and 200 days.

3.10 Pozzolanicity test

The Chapelle test was performed to determine the pozzolanicity of the SCMs used [38]. In this test, 2 grams of CaO was placed in a flask with 1 gram of each of the SCMs at a time. Two hundred and fifty ml of DI water was added to the flask and then it was heated for 16 hrs at 85 °C. After that, the solution was cooled down to room temperature and mixed with 60 g of sucrose as well as another 250 ml of DI water to lower the rate of reaction. Then, the solution was filtered using a vacuum system with a Buchner funnel and a wet filter paper on top. Finally, 25 ml of filtered solution was titrated with 0.1M HCl. The cancelation equation ruling the titration reaction is shown

in Equation 8:

$$N_1V_1 = N_2V_2 \tag{8}$$

Where N_1 and V_1 are the normality number and volume of acid, and N_2 and V_2 are the same parameters for the base. Two reactions occur during titration at the same time as follows (Equations 9 and 10):

$$CaO + 2HCl \rightarrow CaCl_2 + H_2O \tag{9}$$

$$Ca(OH)_2 + 2HCl \rightarrow CaCl_2 + 2H_2O \tag{10}$$

Therefore, in order to determine how much of the $Ca(OH)_2$ has been consumed by the pozzolan, another test was performed with the procedure but without adding any pozzolan. Thus, the decrease in the volume of HCl solution needed for the equilibrium of the titration reaction is an indication of the amount of $Ca(OH)_2$ depleted by the pozzolan. The equation bellow was used for calculations (Equation 11):

$$mg\ of\ Ca(OH)_2\ fixed\ (per\ gram\ of\ pozzolan) = \frac{v_2 - v_1}{v_2} * \frac{74}{56} * 1000 \tag{11}$$

Where v_2 is the volume of HCl solution used for titration of 25 ml of SCM containing solution, v_1 is the volume of HCl solution used for titration of 25 ml of the control solution, 74 is the molecular weight of $Ca(OH)_2$, 56 is the molecular weight of

CaO, and 1000 is for unit correction. The test was performed for all SCMs and the results were used as a comparative measure of their pozzolanicity.

CHAPTER IV

RESULTS AND DISCUSSION

The results of the performed tests will be reported and discussed by possible reasonings.

4.1 Influence of the regenerated SCMs on fresh state properties: Workability

The workability test is an important measure of the fresh state of the mix since fresh state properties would ultimately affect the hardened properties of samples [28]. The flow table results of all samples are presented in Tables 5 to 7. The flow is adjusted by changing SP amounts in order to have similar workability for all mixes.

It was observed that for RM and MK, the flow of the mix decreased as the replacement percentage increased. Therefore, the amount of SP needed for achieving a similar flow with the control sample has increased. Calcined clays generally have higher water absorption due to their higher specific surface and plate like morphology or their rough grain surfaces [39]. Therefore, when they are used as an SCM, they decrease the flowability and increase the viscosity of the mix [40], [41]. More specifically, the workability decrease by the addition of MK as well as the activated EOL materials has been reported by previous studies [42]–[44].

Table 5: Flow table results of MK containing samples

Sample names		*Trial 1 (cm)*	*Trial 2 (cm)*	*Trial 3 (cm)*	*Average*	*SD*
Control	Control	13	15.2	15.5	14.6	1.36
	Control_SP	17.2	17.4	17.9	17.5	0.36
Metakaolin	MK_15	18.2	18.4	18.1	18.2	0.15
	MK_20	16.9	17.5	17	17.1	0.32
	MK_25	17	17.2	17.5	17.2	0.25
	MK_30	18.4	18.2	18.2	18.3	0.11

Table 6: Flow table results of RM containing samples

Sample names		*Trial 1 (cm)*	*Trial 2 (cm)*	*Trial 3 (cm)*	*Average*	*SD*
Control	Control	13.5	14.8	13.8	13.8	0.3
	Control_SP	17.8	19.4	19.7	19	1.02
Red mud	RM_15	18.3	18.4	18.8	18.8	0.55
	RM_20	18.5	19.8	19.4	19.2	0.66
	RM_25	16.5	18.3	17.8	17.5	0.93
	RM_30	18.3	19.3	17	18.2	1.15

Table 7: Flow table results of IZ, MB, NM, and SG containing samples

Sample names		*Trial 1 (cm)*	*Trial 2 (cm)*	*Trial 3 (cm)*	*Average*	*SD*
Control	Control	14.7	15.1	15.1	15	0.23
	Control_SP	17.9	17.7	17.6	17.7	0.15
Izola	IZ_15	17	17	17	17	0
	IZ_20	19.5	18.5	18.2	18.7	0.68
	IZ_25	18.4	18.6	18	18.3	0.30
	IZ_30	18	18.2	18.2	18.1	0.11
Maribor	MB_15	18.7	18.7	18.6	18.7	0.05
	MB_20	17.9	18.7	18.5	18.4	0.42
	MB_25	18.2	18.2	18.4	18.3	0.11
	MB_30	18.7	18.9	18.5	18.7	0.2
Novo mesto	NM_15	17.7	17.5	18	17.7	0.25
	NM_20	18	18.2	18	18.1	0.11
	NM_25	17.7	18.1	18	17.9	0.21
	NM_30	17.9	18.4	18	18.1	0.26
Slovenj Gradec	SG_15	17.6	17.5	17.4	17.5	0.1
	SG_20	17.1	17.9	17	17.3	0.49
	SG_25	17.9	17.7	17.9	17.8	0.11
	SG_30	17.9	17.7	17.9	17.8	0.11

In the case of MK, the decrease in workability depends on many factors such as the amount of the SCM, the source clay, the morphology, and the fineness of this calcined clay [45]. Smaller particles which lead to a higher specific surface would increase water absorption and therefore, reduce the workability. This increases the water demand of the mix, resulting in a dosage of SP. Besides, in MK-based calcined clays, there is more friction between the grains and high electrostatic charge because they have plate-shaped morphology [39]. The rough surface of SCM grains can cause workability reduction, which can be the case also for RM [46]. On the contrary, the other SCMs' samples have similar flowability to plain cement samples. This can be because of their irregular but smooth surface of grains which has low water absorption [47].

Considering the SCM regenerated from construction debris, their influence on workability is less pronounced than both MK and RM. Samples prepared with IZ, NM, MB, and SG exhibited almost similar flow diameters with the control plain mortar regardless of their replacement dosage. In fact, the debris were expected to have a more pronounced impact due to their production method, since they had gone through recycling and grinding process. However, this can be possible that although grinding breaks particles into grains with irregular shapes, but the formed grains have smooth surfaces with low water absorption [47]. Therefore, the lower impact of regenerated debris on workability of the mix can be attributed to their relatively lower water absorption than RM and MK.

Table 8: Flow table results of MK containing samples

Sample names		*Trial 1 (cm)*	*Trial 2 (cm)*	*Trial 3 (cm)*	*Average*	*SD*
Control	Control	13	15.2	15.5	14.6	1.36
	Control_SP	17.2	17.4	17.9	17.5	0.36
Metakaolin	MK_15	18.2	18.4	18.1	18.2	0.15
	MK_20	16.9	17.5	17	17.1	0.32
	MK_25	17	17.2	17.5	17.2	0.25
	MK_30	18.4	18.2	18.2	18.3	0.11

Table 9: Flow table results of RM containing samples

Sample names		*Trial 1 (cm)*	*Trial 2 (cm)*	*Trial 3 (cm)*	*Average*	*SD*
Control	Control	13.5	14.8	13.8	13.8	0.3
	Control_SP	17.8	19.4	19.7	19	1.02
Red mud	RM_15	18.3	18.4	18.8	18.8	0.55
	RM_20	18.5	19.8	19.4	19.2	0.66
	RM_25	16.5	18.3	17.8	17.5	0.93
	RM_30	18.3	19.3	17	18.2	1.15

Table 10: Flow table results of IZ, MB, NM, and SG containing samples

Sample names		*Trial 1 (cm)*	*Trial 2 (cm)*	*Trial 3 (cm)*	*Average*	*SD*
Control	Control	14.7	15.1	15.1	15	0.23
	Control_SP	17.9	17.7	17.6	17.7	0.15
Izola	IZ_15	17	17	17	17	0
	IZ_20	19.5	18.5	18.2	18.7	0.68
	IZ_25	18.4	18.6	18	18.3	0.30
	IZ_30	18	18.2	18.2	18.1	0.11
Maribor	MB_15	18.7	18.7	18.6	18.7	0.05
	MB_20	17.9	18.7	18.5	18.4	0.42
	MB_25	18.2	18.2	18.4	18.3	0.11
	MB_30	18.7	18.9	18.5	18.7	0.2
Novo mesto	NM_15	17.7	17.5	18	17.7	0.25
	NM_20	18	18.2	18	18.1	0.11
	NM_25	17.7	18.1	18	17.9	0.21
	NM_30	17.9	18.4	18	18.1	0.26
Slovenj Gradec	SG_15	17.6	17.5	17.4	17.5	0.1
	SG_20	17.1	17.9	17	17.3	0.49
	SG_25	17.9	17.7	17.9	17.8	0.11
	SG_30	17.9	17.7	17.9	17.8	0.11

4.2 Influence of the regenerated SCMs on fresh state properties: Rheological properties

While mini flow and slump cone tests are simple methods that are commonly used to assess workability, recent advances require a detailed evolution of yield stress and viscosity. Herein, advanced rheological assessment becomes more efficient to determine these rheological parameters. Since the construction debris exhibited similar flow table results, the rheological evaluation was only conducted on those samples containing MK and RM. The results of the rheology tests were evaluated from the flow curves obtained from binder paste samples. Figure 2 shows a representative flow curve for control samples. The remaining flow curves can be found in Appendix B.

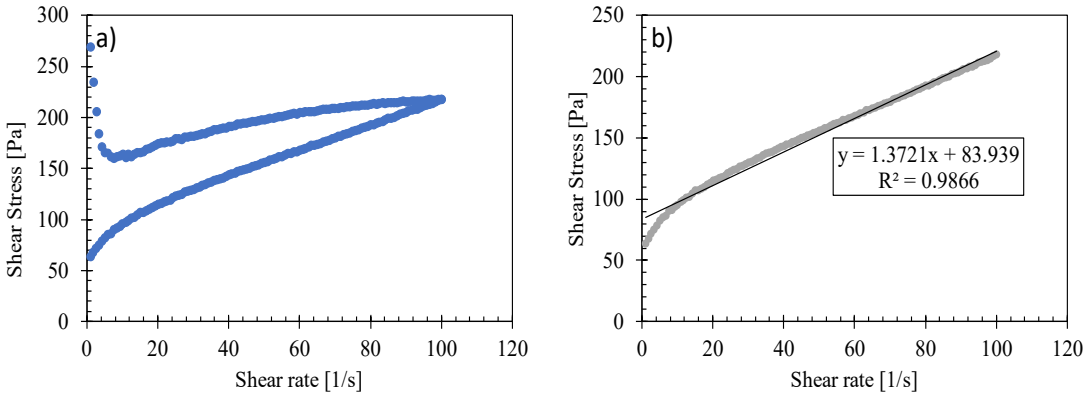

Figure 2: Rheological curve of Control samples a) Full curve, and b) only down curve for regression

A linear regression was applied to the data obtained from the down curve and the rheological parameters were evaluated by Bingham model (see Equation 1 in section 3.4.3). The Bingham rheological parameters are summarized in Table 8.

Table 11: Rheology results of MK containing samples

Sample names		*Dynamic shear stress [Pa]*	*Viscosity [Pa.s]*
Control	Control	83.94	1.37
	Control_SP	50.68	0.69
Metakaolin	MK_15	220.34	1.71
	MK_20	327.17	2.11
	MK_25	535.29	2.84
	MK_30	923.74	3.86
Red mud	RM_15	84.11	1.3
	RM_20	99.23	1.2
	RM_25	160.55	1.44
	RM_30	236.53	1.66

Similar to the flow table results incorporation of MK and RM significantly affected the rheological properties of the mix. The results showed that as the amount of MK and RM increases in the paste, both yield stress and viscosity increase. This observation can be directly correlated to the flow table results [48], [49]. Herein, the decrease in flow table diameter can be attributed to an increase in yield stress. About the

RM samples, the rough surface of this material can cause an increase in the viscosity and yield stress [50]. The smaller particle size of these MK can lead to filling effect which would increase the interaction between particles, leading to a higher yield stress. Besides, higher specific surface which increases water absorption decreases the lubricating effect of water and creates a dryer mix with higher shear strength. Agglomeration of particles can also be another explanation since smaller particles have a higher chance of agglomeration. Besides, when different types of calcined clays are compared, those with higher MK contents increase the yield stress and viscosity more significantly [48], [49]. Generally, since the surface of clays are oppositely charged, the interaction of their surfaces affects the total rheological behavior of the mix and increases their thixotropy. This is due to the fact that clays have a layered structure, in which octahedral alumina and tetrahedral silica layers are connected by exchangeable ions and absorbed water [51] .

Another evaluation that can be done with the flow curves is the thixotropy of the materials. Thixotropy is the ability of the mix to recover its initial viscosity after being thinner under applied shear [52]. The thixotropy can be calculated by determining the area enclosed in the hysteresis from the flow curve (Figure 2-a). For MK samples, as the percentage of MK increases, the down curve gets closer to up curve and the hysteresis area decreases, meaning the thixotropy of the mix increases as the amount of MK increases. Due to the smaller particle size of MK and their filling effect, they would increase the van der Waals forces an structural buildup, leading to a higher thixotropy [53]. However, among the RM containing samples, 20% replacement had the highest thixotropy. Similar to the workability discussion, this can be because of high friction of

RM particles which would favor the thixotropy, while larger particle size works against it [50]. Thus, at 20% replacement there is more balance between these two factors.

4.3 Influence of the regenerated SCMs on rate of hydration: Pozzolanicity test

The pozzzolanicity of RM and MK was measured by the Chapelle test. The results are shown in Figure 3. It is observed that the $Ca(OH)_2$ consumed by the MK is much higher compared to RM. This result is in accordance with compressive strength results, of which it was concluded that RM possess a very low pozzolanic behaviour compared to MK. Although RM contains the oxides needed to be a potential pozzolan regarding ASTM and ABNT standards (SiO_2, Al_2O_3, and Fe_2O_3) but it shows low pozzolanic activity. Similar results were also obtained in previous studies [43], [54]–[57]. The low pozzolanic behaviour of RM was attributed to low amounts of active silicon and aluminium present in the mix which are supposed to be supplied by the decomposition of pozzolanic materials and are the main force in pozzolanic activity [58], [59]. It is noteworthy that apart from intrinsic characteristics of the material, the activation method/temperature and the alkalinity of the cementitious environment they are being added to, are two main factors affecting the pozzolanicity of those materials [56].

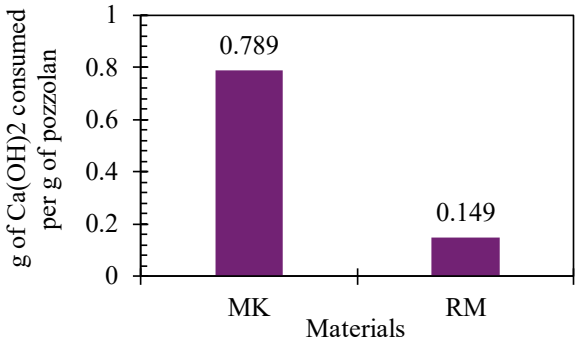

Figure 3: Chapelle test results

4.4 Influence of the regenerated SCMs on rate of hydration: Initial Setting

The influence of regenerated EOL and MK was then assessed in terms of initial setting. Table 9 summarizes the average initial setting times recorded for each cement paste sample.

Table 12: Initial setting results of MK containing samples

Sample names		*Trial 1 (min)*	*Trial 2 (min)*	*Average*	*SD*
Control	Control	505	475	490	15.00
	Control_SP	825	810	818	7.50
Metakaolin	MK_15	605	620	613	7.50
	MK_20	540	560	550	10.00
	MK_25	475	495	485	10.00
	MK_30	440	450	445	5.00
Red mud	RM_15	700	710	705	5.00
	RM_20	635	630	632	2.50
	RM_25	380	370	375	5.00
	RM_30	180	175	177	2.5
Izola	IZ_15	750	755	753	2.50
	IZ_20	745	760	753	7.50
	IZ_25	755	745	750	5.00
	IZ_30	760	760	760	0.00
Maribor	MB_15	840	825	833	7.50
	MB_20	875	860	868	7.50
	MB_25	910	885	898	12.50
	MB_30	900	900	900	0.00

Table 9: Initial setting results of MK containing samples (continued)

Sample names		*Trial 1 (min)*	*Trial 2 (min)*	*Average*	*SD*
Novo mesto	NM_15	790	775	783	7.50
	NM_20	820	835	828	7.50
	NM_25	870	855	863	7.50
	NM_30	800	795	798	2.50
Slovenj Gradec	SG_15	790	775	783	7.50
	SG_20	780	770	775	5.00
	SG_25	795	825	810	15.00
	SG_30	850	855	853	2.50

Herein, it should be noted that the amount of SP in the mixes were kept the same to make a fair comparison among the samples. First of all, the use of SP in Control_SP sample resulted in a longer setting time compared to control sample prepared with only water and cement. This is expected due to the working mechanism of superplasticizers. Superplasticizers are polymers that create a temporary barrier around cement particles which would disperse them (increase workability) and hinder their dissolution (increase setting time) [60].

Incorporation of both RM and MK decreased the setting time compared to Control_SP sample. However, the increase in rate of hardening and setting cannot be correlated with the rate of strength development. With the relatively smaller particle size MK generally increases the rate of hydration [48]. This also affects the rate of

strength development and can lead to higher strength development staring from 3-days [48]. This can be explained by the filler effect of SCMs that have smaller particles which fill a portion of the voids, creating a more compact environment and increase the friction resisting needle penetration. In addition, finer particles increase to total surface area available for nucleation of cement hydrate, leading to accelerated initial setting. Another reason leading to such decrease in setting time with MK addition can be the high water absorption capacity of MK resulting in the formation of hydrates also occurs faster [57].

A similar trend was observed in samples containing RM. In fact, incorporation of 30% RM resulted with the shortest setting time among all the samples. Considering the influence of RM on setting time and relatively lower pozzolanicity, this effect can be explained by its similar nature to Calcium Aluminate Cements (CAC). RM samples contain high alumina content similar to CACs, and decreased setting time has also been observed in CACs [61]. Therefore, RM mixes show similar behaviour to CACs in terms of setting time. Although this fast reaction of high aluminate binders with water increases the setting rate of the mix, but the rapid formation of hydrates leads them to have unorganized structures which affect their long-term performance.

For the construction debris samples (IZ, MB, NM, and SG), the setting time has slightly increased compared to the Control_SP sample regardless of the type. Similar to the flow table results, lower water absorption of these materials might have decelerated the formation of hydrates. Another explanation can be that although in all EOL-containing pastes, there is less hydrates available to cause the initial setting, but RM grains have a rougher surface and there is more friction between particles that could

help with resisting needle penetration. However, construction debris have smooth grain surface as discussed in workability test results (see section 4.1).

4.5 Influence of regenerated EOL on hardened properties: Compressive strength

The compressive strength results are depicted in Figures 4 to 9. In addition, the compressive strength of SCM containing samples is compared to control samples by finding their relative strength percentages. These percentages are presented in Tables 10 to 12.

It is noticed that up to 20% MK replacements can increase the strength of the samples after 28 days of curing. Three reasons can explain this phenomenon [62], [63]. First, smaller particle size of MK causes a filler effect which decreases the void ratio by filling them with lead bearing solids and creates a more compact sample which can resist higher loadings. The filler effect is influential from the beginning. Second, smaller particles that have higher specific surface also have higher dissolution rate, which increases the hydration speed [48]. The third and the main reason is the pozzolanic reaction in which the CH phase is turned into strengthening C-S-H phase [14]. The pozzolanic reaction which can continue up to 180 days. The strength enhancement by using MK has been reported in several studies before [64]–[66]. MK is the best calcined clay in terms of pozzolanic reactivity. It is claimed that when different grades of calcined clays are included in a mix, the most important factor affecting the strength is the MK content of the calcined clay [65], [67]. However, for higher replacements

percentages, the strength decreases. One reason can be that with higher MK in the mix there is lower cement available for forming CH phase to be converted into C-S-H.

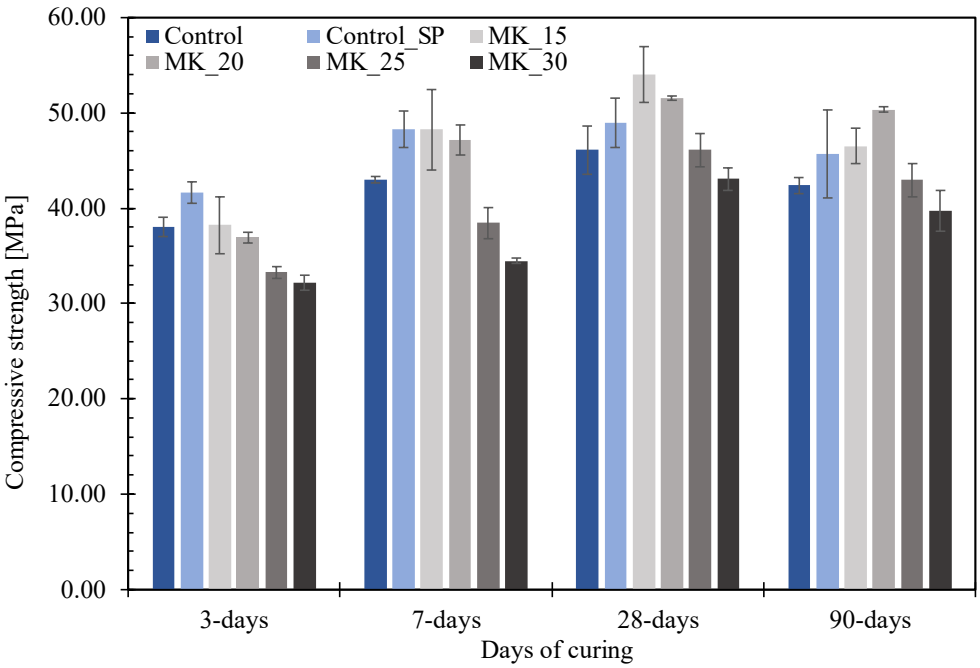

Figure 4: Compressive strength results of MK samples

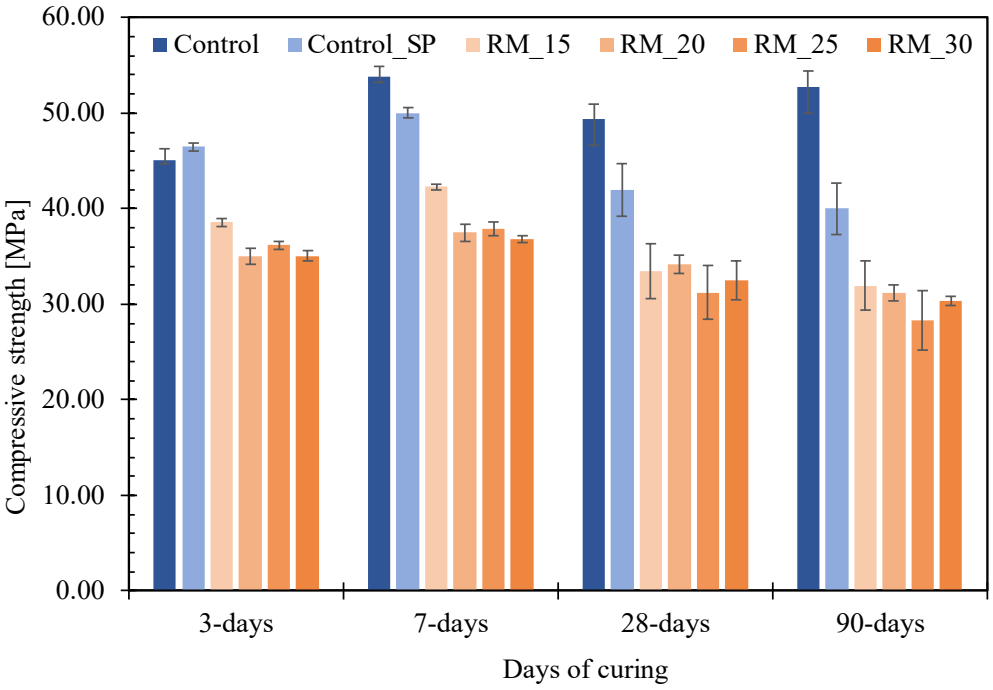

Figure 5: Compressive strength results of RM samples

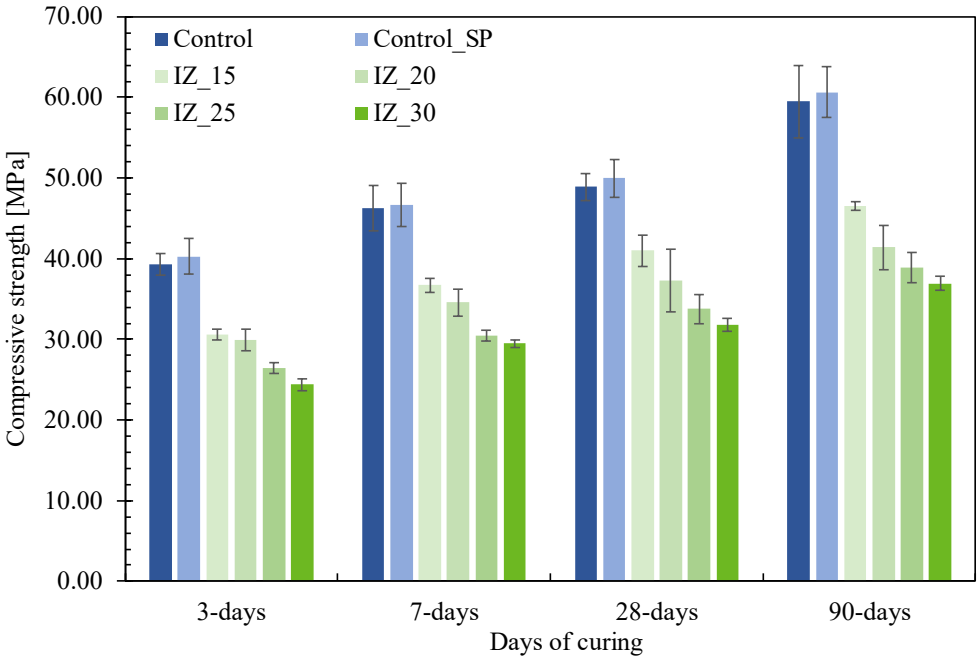

Figure 6: Compressive strength results of IZ samples

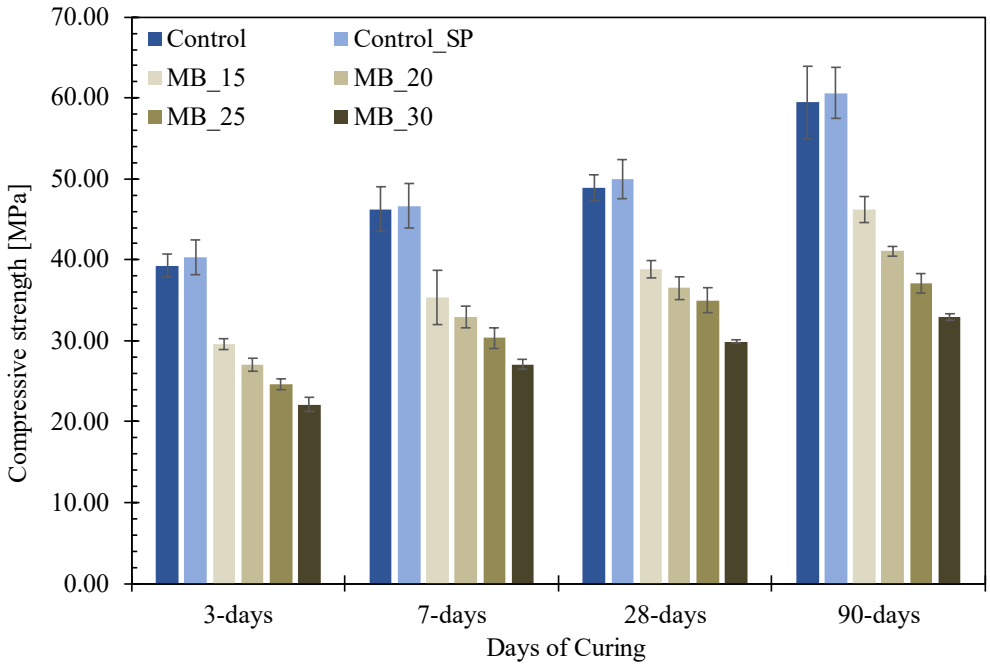

Figure 7: Compressive strength results of MB samples

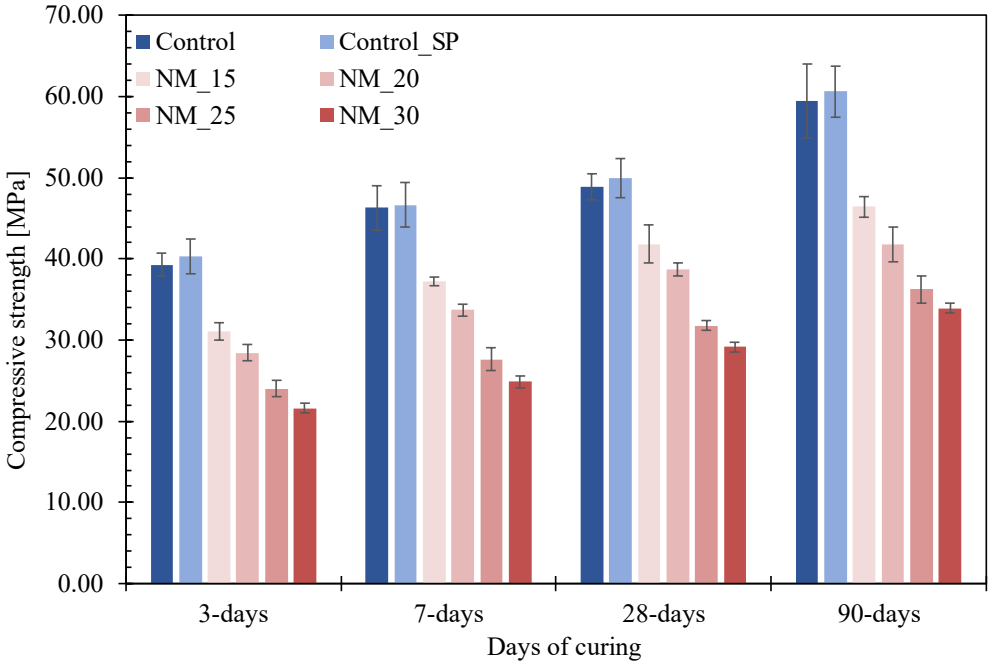

Figure 8: Compressive strength results of NM samples

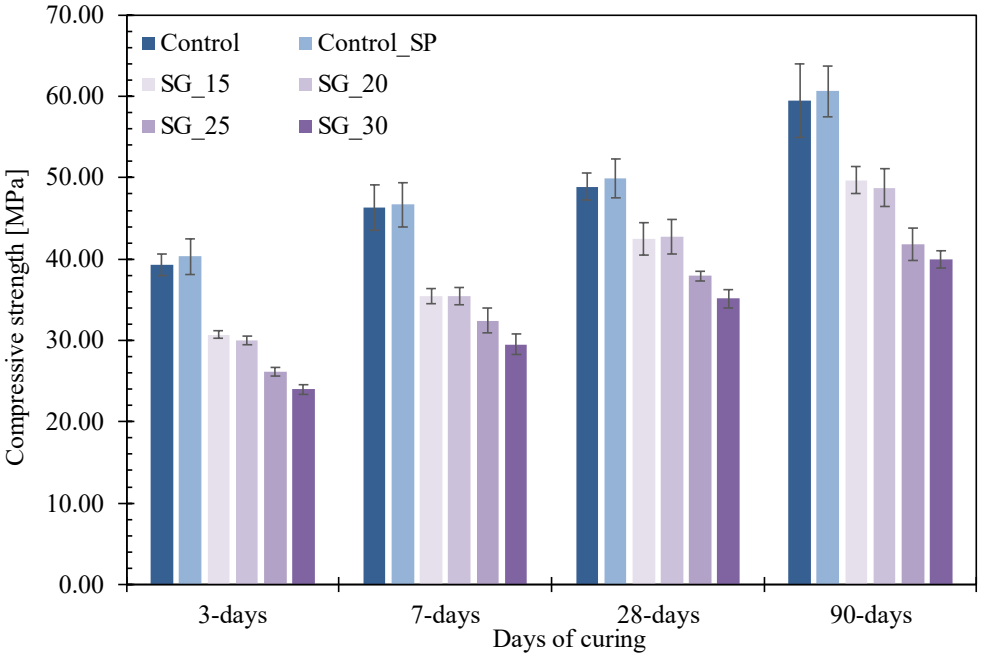

Figure 9: Compressive strength results of SG samples

Table 13: Relative strength of MK containing samples

Sample names	*% strength in relation to Control_SP at different ages*			
	3 days	*7 days*	*28 days*	*90 days*
MK_15	91.86	98.94	110.41	101.92
MK_20	88.72	97.57	105.33	110.30
MK_25	80.00	79.66	94.15	94.07
MK_30	77.29	71.39	87.99	86.91

Table 14: Relative strength of RM containing samples

Sample names	*% strength in relation to Control_SP at different ages*			
	3 days	*7 days*	*28 days*	*90 days*
RM_15	81.37	84.54	79.76	79.87
RM_20	74.72	74.90	81.55	77.92
RM_25	75.77	75.78	74.45	70.76
RM_30	73.56	73.65	77.59	75.87

Table 15: Relative strength of IZ, MB, NM, and SG containing samples

Sample names	*% strength in relation to Control_SP at different ages*			
	3 days	*7 days*	*28 days*	*90 days*
IZ_15	76.75	78.65	82.04	76.67
IZ_20	75.01	74.07	74.61	68.27
IZ_25	66.58	65.25	67.55	64.23
IZ_30	61.77	63.18	63.18	60.91
MB_15	74.24	75.68	77.82	76.22
MB_20	68.28	70.60	73.07	67.77
MB_25	62.34	64.98	70.00	61.24
MB_30	56.26	58.06	59.89	54.35
NM_15	77.87	79.88	83.70	76.59
NM_20	71.45	72.20	77.45	68.90
NM_25	60.91	59.26	63.66	59.81
NM_30	55.12	53.30	58.37	55.97
SG_15	76.98	75.90	85.13	81.98
SG_20	75.17	75.96	85.56	80.48
SG_25	65.99	69.50	75.95	68.92
SG_30	60.76	63.26	70.40	65.93

For all the other SCMs used in this study, the addition of SCM has decreased the strength of the samples. However, it has been observed in the previous studies that up to 10% RM replacement can increase the strength [68]. But among the mix designs used in this study, none of them were able to compensate for the lower amounts of cement available in the mix. The most probable explanation is that when recycled SCMs are added to the mix, the hydratable component volume decreases, forming lower amounts of both CH and C-S-H [69]. And unlike MK samples, this decrease has not been compensated by pozzolanic reaction at later days. As discussed in section 4.4, RM samples have similar behaviour to CACs from initial setting and hydration reaction aspect because of high aluminate content of both materials. This rapid reaction forms weak and disorganized forms of the aluminate hydrates (such as strätlingite) [70]. Thus, the mix does not have as much strength as control samples. Besides, it has been mentioned that the SCMs that have high water absorption, most of the water available in the mix is used for wetting the surface of grains, leaving not enough water for hydration [71]. This can be true for RM samples in this study. Besides, SCM particles can agglomerate around cement grains and hinder their dissolution and hydration, which can apply to all SCMs used in this study and MK at high replacement percentages [71]. The RM and debris samples increase the amount of CaO or free lime in the mix. This can decrease the strength of the mix because of expansion and formation of excess CH [72]. The RM containing mixes have had similar hydration process to calcium aluminate cement [73], [74]. The aluminate phase formation is more pronounced in these mixes leading to lower strength values. In addition, the amount of gypsum present in the mix

may not be enough to control the hydration reaction of high amounts of aluminate phases, which would lead to low strength values.

There are a number of standards regarding usage of SCMs in mortar or concrete mixes in terms of the compressive strength of samples. ASTM C618 standard mentions SCM containing samples must have at least 75% of the strength of the control samples at 7 and 28 days [55]. This percentage is mentioned to be 70% in other sources [75], [76]. Then, it is lowered to 65% at only 28 days in Chinese National Standard GB/T 2847-2005 [77]. Other sources have mentioned at least 28 MPa for hydraulic cement for construction applications and 25 MPa for high sulfate resistant cement [78], [79]. Most of the mix designs used in this study satisfy these standards for compressive strength. While these samples might not be suitable for structural applications there could be other applications where we can benefit from these mixes, such as for temporary standing/loading situations, when rapid hardening is needed in tunnel caving as an example, for modifying setting and rheology of printable concrete, and for strengthening base/sub base of pavements.

4.6 Compressive strength estimation method using multiple linear regression

A series of multiple linear regression equations were developed relating the compressive strength to mix design and to curing age are presented in this section (Equations 12, 13, 14, 15, 16, and 17). The equations represent compressive strength of MK, RM, IZ, MB, NM, SG respectively (the parametric equation is shown in Equation 4):

$$y_{MK} = 0.1442\,(MK) - 1.3846\,(SP) + 0.0430\,(Age) \quad R^2 = 27\% \tag{12}$$

$$y_{RM} = -0.5832\,(RM) + 0.1821\,(SP) - 0.0633\,(Age) \quad R^2 = 77\% \tag{13}$$

$$y_{IZ} = -0.6297\,(IZ) - 0.5013\,(SP) + 0.1433\,(Age) \quad R^2 = 94\% \tag{14}$$

$$y_{MB} = -0.6531\,(MB) - 1.2199\,(SP) + 0.1430\,(Age) \quad R^2 = 94\% \tag{15}$$

$$y_{NM} = -0.7488\,(NM) - 0.3253\,(SP) + 0.1453\,(Age) \quad R^2 = 95\% \tag{16}$$

$$y_{SG} = -0.5686\,(SG) - 0.5739\,(SP) + 0.1741\,(Age) \quad R^2 = 92\% \tag{17}$$

Based on the R^2 values, it is observed that these equations have acceptable accuracy, except for MK. This is because the strength of MK samples increases with increase in the MK samples up to a certain percentage and then decreases. Besides, this pattern is not exactly followed at different ages. Thus, a linear relation does not exist between the changing parameters. For other SCMs, it is noticed that SCM percentage has a negative coefficient which means when other conditions are constant, the strength decreases as the SCM percentage increases. This coefficient is bigger for NM, which decreases the strength the most. The coefficient of SP content also has a negative sign. It should be noted that in practice SP content increases the strength because of better

compaction. This negative sign appears because in this study, higher SP amounts were used in mixes with higher SCM replacements. And, since those mixes had smaller strength values, SP content has a minus sign in equations. This is does not apply to RM equation because of strength value fluctuations with increase of SP.

4.7 Compressive strength estimation method using Artificial Neural Network (ANN)

A MATLAB code was used for this estimation and the code is shown in Appendix C. The model has one hidden layer is chosen with 7 neurons. 87 percent of the data points (number of 21 data points) were used as training data and 13 percent (number of 3 data) were used as validating data. The number of neurons was chosen such that Root-mean-square error (RMSE) values were the lowest for both training and validating data. In the final run the RMSE values were under 2 MPa for all materials (Table 16). In general, the RMSE value of training data should be greater than the RMSE value of validating data, which is an indication of a good fitting and not over fitting.

The results of the ANN model are related to experimental results in Figures 10 to 15. The equations shown on the figures show how good the relationship is between estimated and actual strength values. For all cases, the slope of the line for training data is very close to one and the R^2 values are all higher than 0.9. It is observed that ANN results have better agreement with experimental results compared to linear regression model. Especially for the MK which had non-linear relationship between variables. This

is the strength of ANN method. While in regression model, being able to see the coefficients of variable gives good understanding of the relationship between variables.

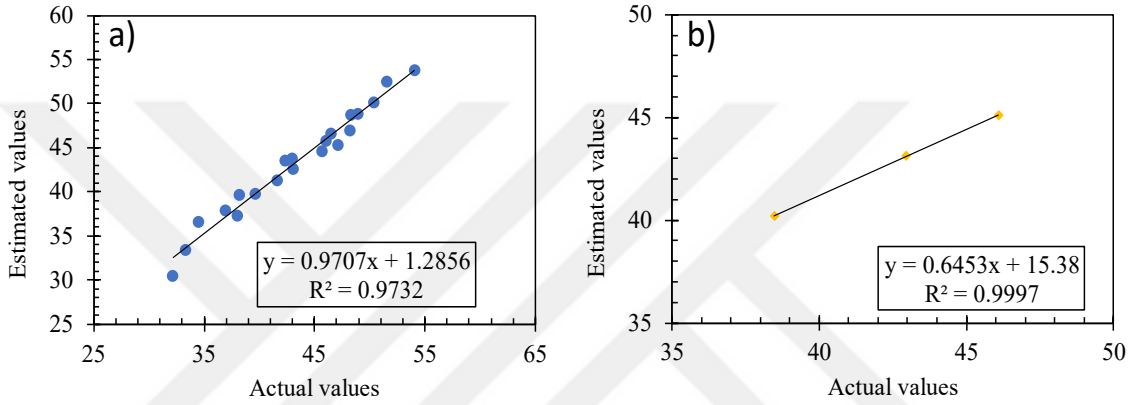

Figure 10: ANN results of MK samples: a) Training data, and b) Validating data

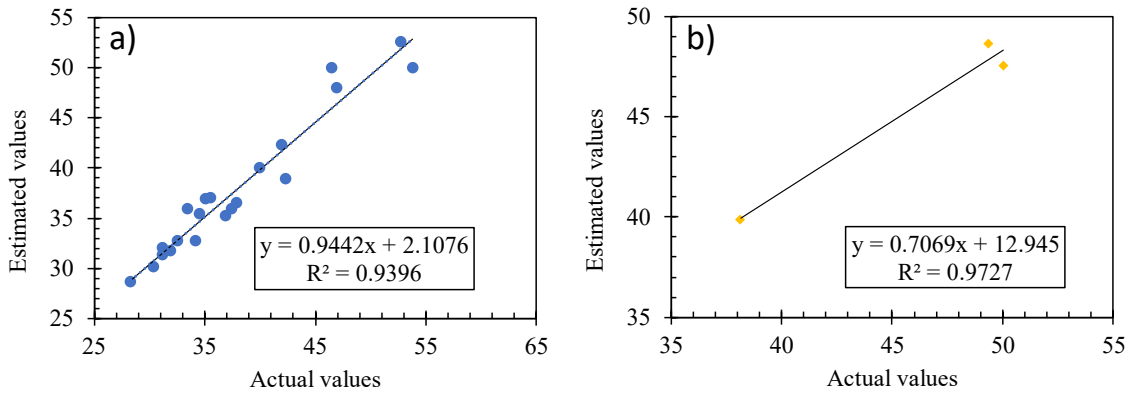

Figure 11: ANN results of RM samples: a) Training data, and b) Validating data

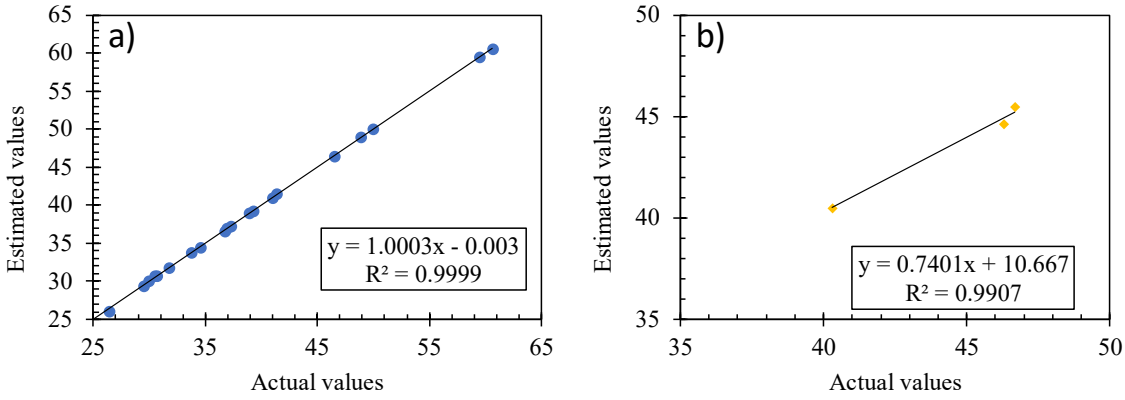

Figure 12: ANN results of IZ samples: a) Training data, and b) Validating data

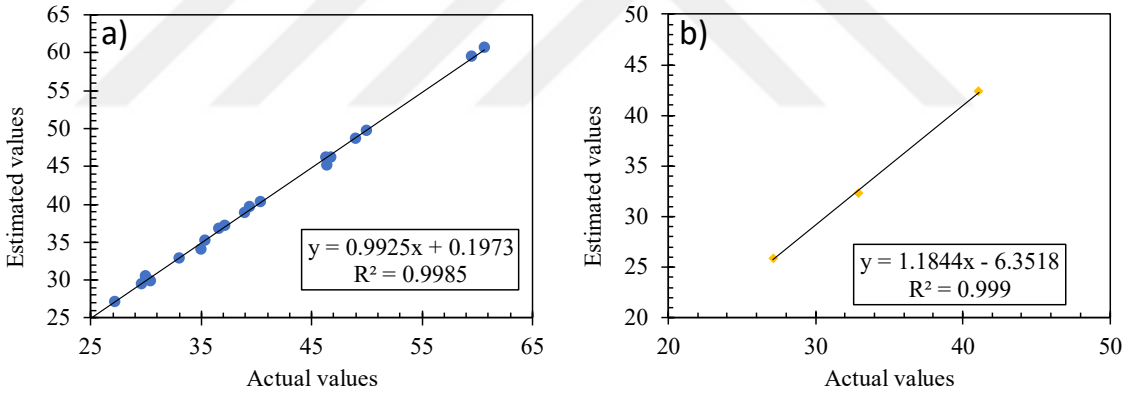

Figure 13: ANN results of MB samples: a) Training data, and b) Validating data

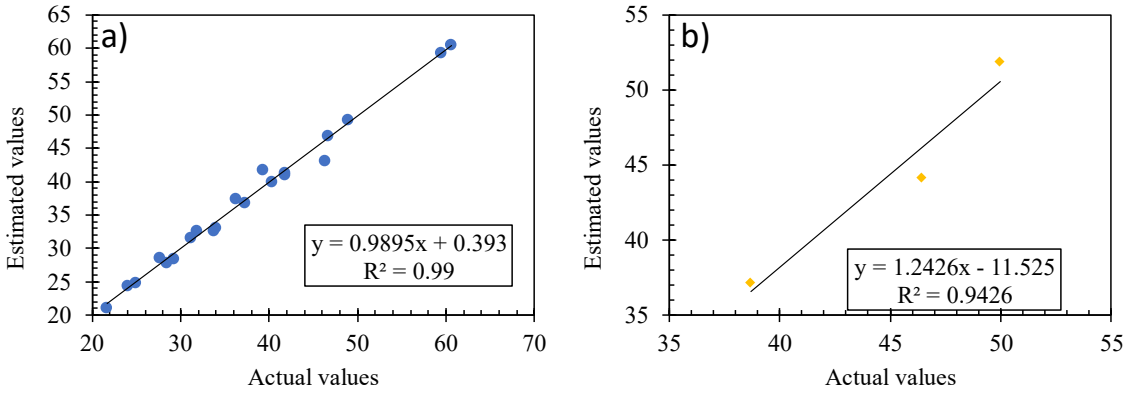

Figure 14: ANN results of NM samples: a) Training data, and b) Validating data

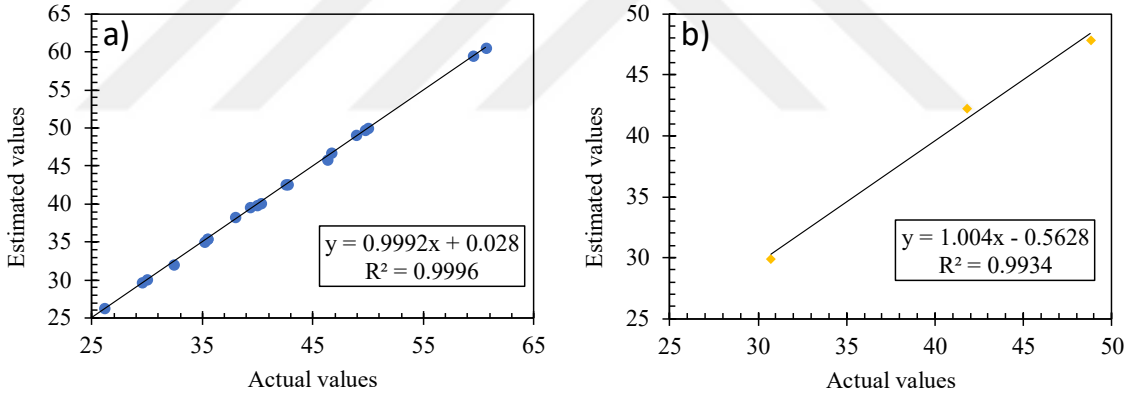

Figure 15: ANN results of SG samples: a) Training data, and b) Validating data

Table 16: RMSE results of ANN models

Sample names	*RMSE of training data*	*RMSE of validating data*
MK	0.9898	1.1503
RM	1.7434	1.6316
IZ	0.1186	1.1787
MB	0.4169	1.0873
NM	1.0452	1.9363
SG	0.1884	0.7310

4.8 Water absorption

Water absorption occurs when moisture penetrates through capillary absorption in pores [41], [80]. Because water absorption is a major property that controls transport of deteriorating materials into the sample, it has a great impact on the durability of concrete [81]. When SCMs are incorporated in concrete mix, they can decrease the porosity and therefore can reduce water absorption capacity. The results of water absorption test are presented in Figure 16.

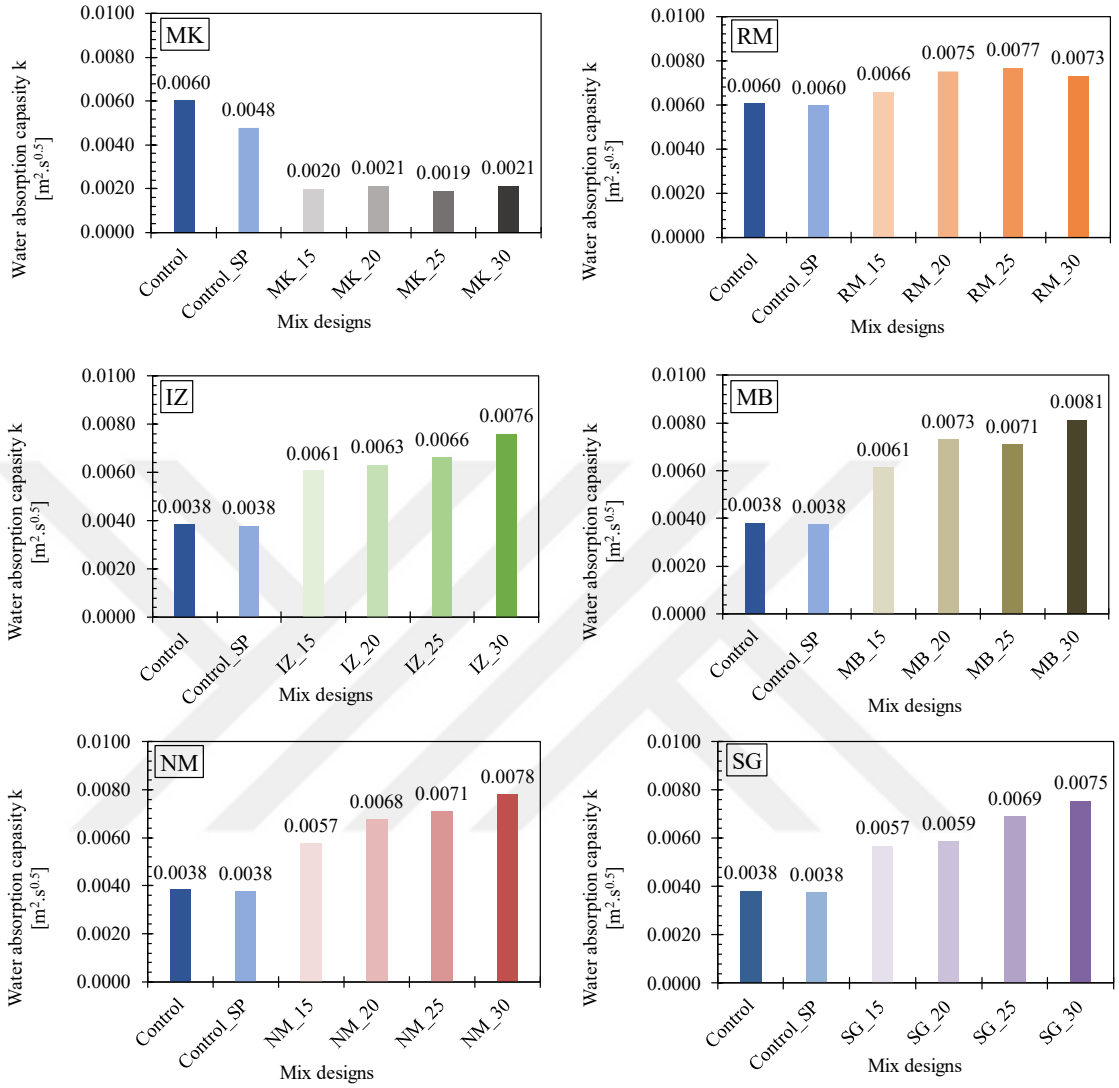

Figure 16: Water absorption results

It is observed that addition of MK decreased the water absorption capacity. This could be because of the filler effect of smaller MK particles which plugs a portion of voids, especially in the interfacial transition zones [82]. On the other hand, pozzolanic reaction also can help with decreasing porosity by forming more C-S-H phase. Because of these reasons, the MK containing samples have a more compact and cohesive

structure with lower space for water transport, which agrees with compressive strength results. On the contrary, other samples containing regenerated EOL have higher water absorption than control samples. One reason can be that since there is less hydrated products because of lower cement content, the structure is more porous [46]. Besides, for RM case, since it has a porous nature itself, it has a higher specific surface to which water has access [83]. This structure can absorb and hold water inside the mix. In addition, including recycled SCMs inside samples increases disorganization which can lead to formation of micro cracks, and in turn, increases the water absorption [84], [85]. Considering the flow table, setting time, and strength results, lower hydrates and micro cracks is a more probable explanation. Slight fluctuations among the results for different SCM percentages can come from the fact that not all of the mix designs had same flowability results, therefore they might have had compaction variations.

4.9 Sulfate attack

The results of the sulfate attack test are shown in Figure 17. For this test, only 25% cement replacements were used, and the samples were introduced to sulfate environment at an early age of 2 days.

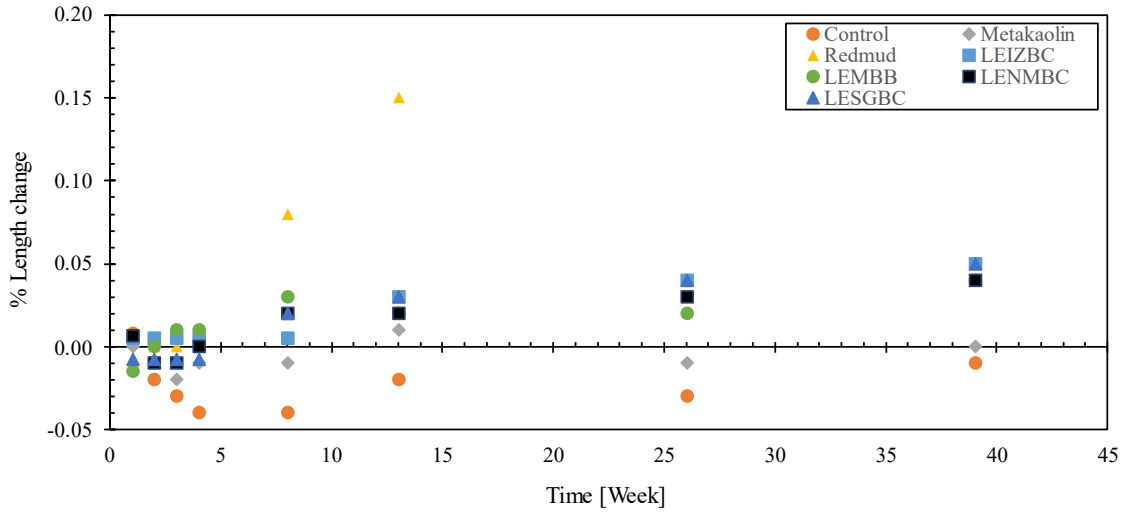

Figure 17: Sulfate attack test results

It is observed that among SCM containing mixes, RM sample has the highest and MK has the lowest expansion. High amounts of aluminate phases in RM and existence of limestone in the debris samples increases the formation of monocarboaluminates. Since CH phase also exists, in a sulfate environment, high sulfate ettringite forms. The expansion caused by ettringite formation would create cracks that increase sulfate penetration to the samples. This would cause CH phase to form gypsum with sulfate, which would decrease the consistency of the sample and eventually causes deterioration. RM samples had the most severe reaction in the solution. They expanded the most and were broken to pieces after 15 weeks exposure (Figure 18).

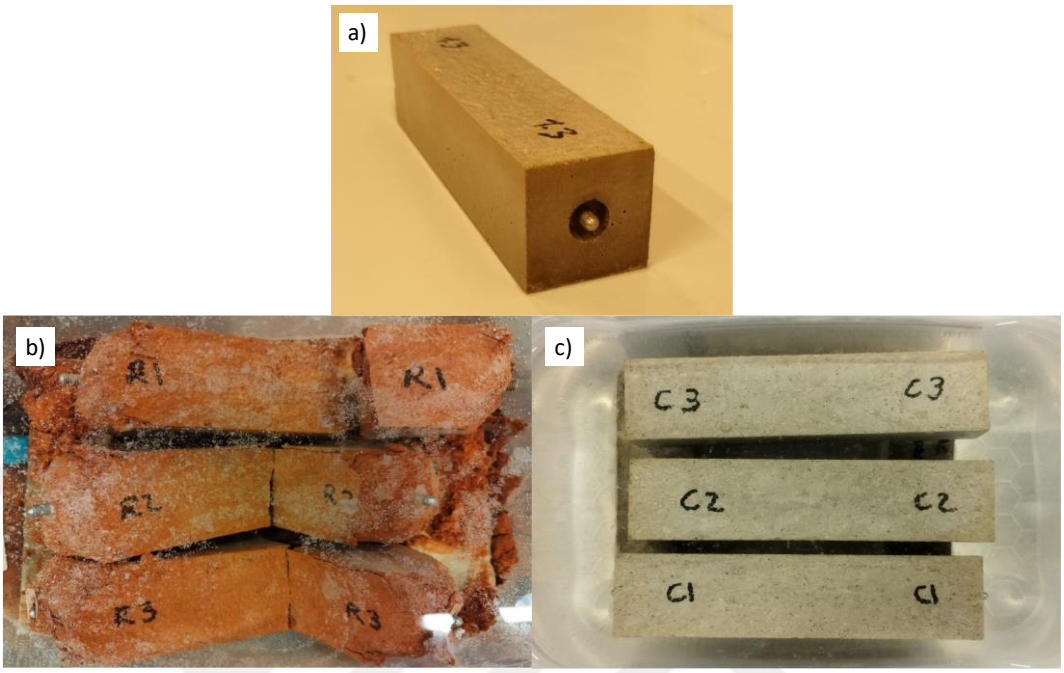

Figure 18: Sulfate attack samples: a) General samples of length changing beams, b) RM samples at 15 weeks, and c) Control samples at 15 weeks

Similar to its hydration process, in this test also RM behaviour is similar to aluminate cement [74]. The vulnerability of concrete to sulfate environment increases as C_3A content increases. Higher ettringite formation, early gypsum depletion, and lower cement content and C-S-H phase all contribute to deterioration of RM samples [86]. About the debris SCMs, they contain a percentage of limestone which would increase monocarboaluminate phase and initiate sulfate deterioration [87]. The expansion of MK sample is higher than control sample. However, since the water absorption results of MK samples were lower than control samples, it was expected that the ions for deterioration have lower access to the structure of MK samples, and therefore, the expansion was expected to be lower than control samples [88], [89]. However, control

samples also have shown zero expansion similar to metakaolin samples. It has to be considered that the water absorption test was performed after 28 days of curing, when the pozzolanic reaction was initiated and the increase of C-S-H phase had filled a portion of pores. But for the sulfate attack test, the samples were placed in the sulfate solution after only two days of moist curing. When control samples are placed in the solution, there is more hydrated cement phase of C-S-H which can resist the harsh environment. Besides, the compressive strength results also show that the C-S-H formation in 25% MK samples is not more than control samples. These reasons can balance the condition of sulfate resistance for control and MK samples. In addition, as the cement content in a mix decreases, the expansion from sulfate attack increases [90].

4.10 Alkali Silica Reaction (ASR)

Another common durability problem that can occur in cement-based systems is ASR. The ASR occurs when alkalis (such as sodium) come in contact with reactive silica (coming from aggregates) and form a gel that swells in presence of water. This swelling would then apply internal pressure which would cause expansion and cracks, and ultimately, spalling of the concrete. The ASR test results are presented in Figure 19.

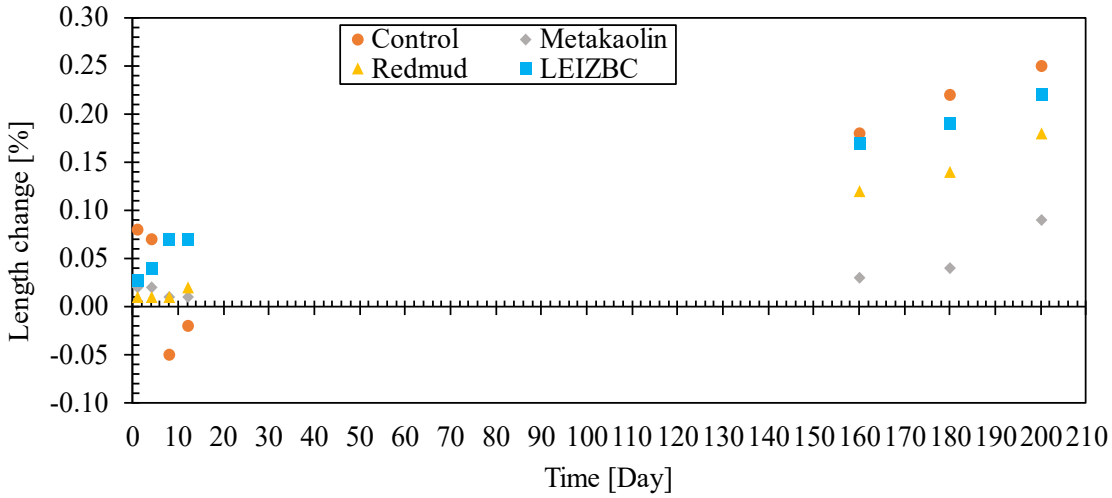

Figure 19: ASR test results

Herein, the control samples without any SCMs showed the highest amount of expansion, suggesting that these SCMs contributed to mitigating ASR regardless of their pozzolanic potential. As stated in the literature and proved in water absorption and compressive strength tests, pozzolanic reaction in MK samples converts CH phase into C-S-H phase.

It is mentioned in the previous studies that the expansive gel related to ASR has high Ca^{2+} [91]. This cation is believed to come easiest from CH phase which is less stable and more active than C-S-H phase. On the other hand, the ASR depends on the active silica existing in the aggregates, and since the aggregates used in this study are same for all samples, the changing parameter among different mix designs is the amount of CH. Therefore, the ASR expansion is most related to the CH to SiO_2 (active) ratio. Incorporation MK can decrease the ASR explanation by decreasing the amount of

CH and decreasing the permeability of samples. In a holistic point of view, MK can eliminate the 3 main components of ASR reaction.

Even though, RM containing samples did not perform as good as samples containing MK, incorporation of RM to the mix mitigated the ASR expansion. The relatively lower performance of RM over MK can be explained by its lower pozzolanic activity. Nevertheless, RM can actually decrease the amount of CH in the mix by triggering latent pozzolanic reaction.

The samples containing SCM regenerated from construction debris contain a percentage of limestone, which would increase the alkalinity in the pore solution which makes the ASR more severe [92]. The IZ samples have more expansion than RM samples since RM samples have more aluminate phases and lower CH phase. Besides, RM and IZ samples had higher water absorption, and therefore, higher porosity. Although this would help solution entrance into the samples, the higher porosity creates more space for reaction products which can decrease expansion [93].

CHAPTER IV

CONCLUSION

In this study the regeneration potential of EOL materials were studied and the performance of concrete mixes produced using these materials was tested with various methods. First the materials were selected, ground, and heat treated. The treatment temperature was determined by characterization tests such as TGA and XRD. After regeneration, the materials were included in mortar mixes. In these mixes, certain amounts of cement were replaced by one of the SCMs. Different replacement percentages were examined in order to understand the relation between amount of these SCMs and changes in the properties of concrete. These percentages were 15, 20, 25, and 30 percent. The performance tests can be divided into three steps.

In the first step, the fresh state properties of mixes were studied. The fresh state tests were workability test, setting time determination test, and rheology test. For workability, flow table test was performed. It was observed that RM and MK significantly decrease the flow of the mix, while debris SCMs had little or no decreasing effect on flow of the mix. High water absorption, filler effect, and high friction between grains can be a reason for workability decrease by addition of RM and MK. However, the morphology of debris samples led to their lower water absorption and almost similar flowability with control samples. The RM and MK containing pastes were further studied using rheology tests. It was observed that RM and MK increase viscosity and shear resistance of the mix. Layered structure of clays and smaller particle size of MK, as well as higher friction and lower free water available for lubrication in RM

containing pastes are the probable causes for these results. The initial setting time was also decreased substantially as the amount of RM and MK increased in the binder paste. Other SCMs had little and fluctuating effect on initial setting time of the mix. Because of the high aluminate phase content in RM, the samples performed similar to CACs. The reason of faster setting of MK containing samples was their smaller particle size which accelerates the hydration and causes a filling effect. Since IZ, MB, NM, and SG did not change these properties significantly, their setting time was close to control samples.

The hardened properties of the mixes were investigated by the compressive strength test. The test was performed after 3, 7, 28, and 90 days of curing. It was observed that MK increases the compressive strength up to 20% replacement. This was expected as MK was used as a reference representing the performance of best-known calcined clay. High pozzolanic reaction of MK is the main reason for this result. Other SCMs used in this study showed limited pozzolanicity and decreased the compressive strength as their amount increased in the mix. For RM containing samples, rapid setting with similar behaviour to CACs has probably created weak and disorganized aluminate hydrates that had low contribution to strength gain. Also, the regenerated construction debris probably had low amounts of hydratable phases which caused strength decrease in those samples. However, the obtained strength values of all SCMs satisfied several standards for using SCMs in concrete mixes. For the compressive strength, regression equations and ANN models were developed for estimating the strength of other replacement percentages between 15 and 30 percent.

In the third step, tests related to durability of mixes in different environment were studied. One of the most important properties affecting the durability of concrete

is the permeability of it. Thus, the water absorption of samples was measured. Among the used SCMs in this study, the MK decreased the water absorption while other SCMs increased it. This is mainly due to pozzolanic reactions in MK samples that created denser structure than other samples. For the other durability test, length changing samples were prepared and introduced to two different harsh environments for sulfate attack and ASR. All SCMs helped with decreasing the expansion from ASR because of the pozzolanic activity or lower amounts of active ions needed for the reaction. For the sulfate attack test, all SCMs had acceptable performances except RM which spalled during the test because of high amounts of aluminate phases.

In conclusion, the results from all the performed tests were in consistency and showed low pozzolanic activity of all re-generated EOL materials. However, these materials can be used for special and non-structural applications; they can replace cement in ready-to-use/non-load-bearing panels, they can be used as temporary and fast hardening barriers during construction works such as tunnel carving, they can provide additional stability of base and/or subbase of pavements, and they can act as rheology and/or setting time modifiers in 3D printing of concrete.

5.1 Future works

Since the idea of using regenerated EOL materials as SCMs has numerous benefits, increasing the number of EOL sources to be tested can be one of the future works of this study. In addition, similar to geopolymer concrete, using chemical activation methods may also increase the reactivity of EOL materials which can be investigated. Besides, comparing all the results of RM with CAC samples for a more detailed comparison is of great potential benefit since partially replacement of CAC

with RM agrees with the environmental aim of this study. Using the SCMs in the above-mentioned non-structural application and studying their performance is also another future work. This can be further improved by life-cycle-assessment and sustainability investigation in order to fully understand the possible benefits.

APPENDIX A:
Source identification, characterization, and regeneration of SCMs

Raw cement was received from ÇimSA and AkcanSA Cement Manufacturing Company (Istanbul, Turkey). This cement was preferred as type I and 42.5 R (Figure 20). The MK used in the study was a commercial ready to use material. Wet RM sample was received from the ETI Aluminum Manufacturing (Konya, Turkey) (Figure A.1). Before performing a characterization analysis, RM was dried at 100 ºC oven furnace and grinded in each process. The construction debris were obtained from four different waste disposal sites in Slovenia, namely Slovenj Gradec (SG), Maribor (MB), Izola (IZ), and Novo mesto (NM). These sources were old hydrated cement and cement separated from concrete waste. These materials were crushed and large pieces such as aggregates were removed. Then, in order to obtain particle size of 45 μm fraction, the materials were ground in a MILMIX 20 ball mill for 1 minute and 50 s at 25 round per second. Heat treatment method for red mud sample: 300 ºC for 1 hour and 850 ºC for 2 hours.

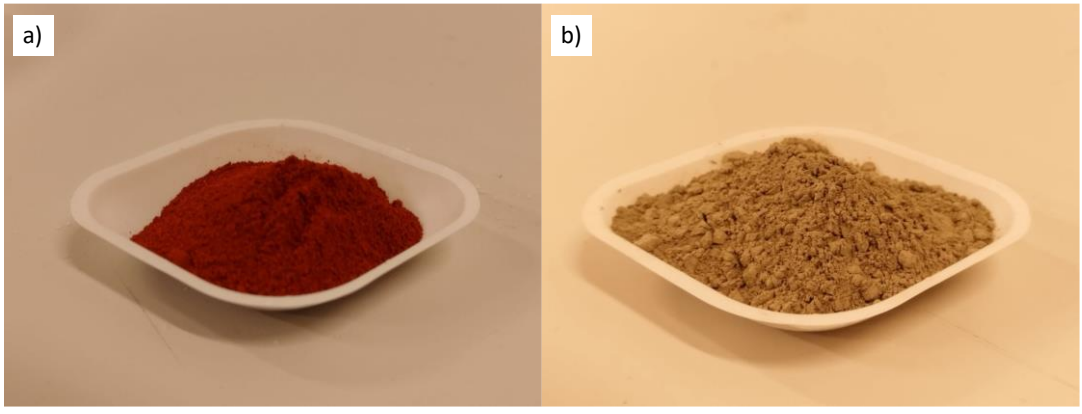

Figure 20: Samples of a) Red mud, b) OPC

In TGA analysis, the weight change of powdered samples was measured while being heated. RM samples were heated up to 1000 ℃ (Figure 21). The TGA machine used for construction debris was STA 449 Jupiter from NETZSCH. The heating temperatures were 800 ℃, 900 ℃, and 1100 ℃ with 3 hours waiting at each (Figures 22 to 25). The particle size of the powder at 800 ℃ was under 100 nm, at 900 ℃ was ~270 nm, and at 1100 ℃ it was sintered. The first and biggest weight loss of RM at around 300 °C is associated with the dihydroxylation of Gibbsite. For the construction debris, the main peaks at 800 °C- 900 °C are related to Calcite and limestone.

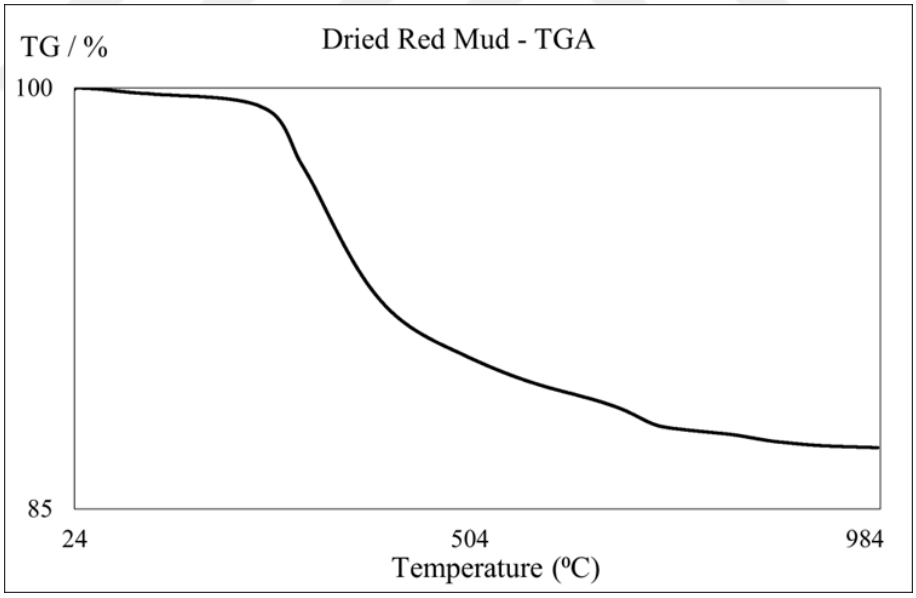

Figure 21: TGA results of RM

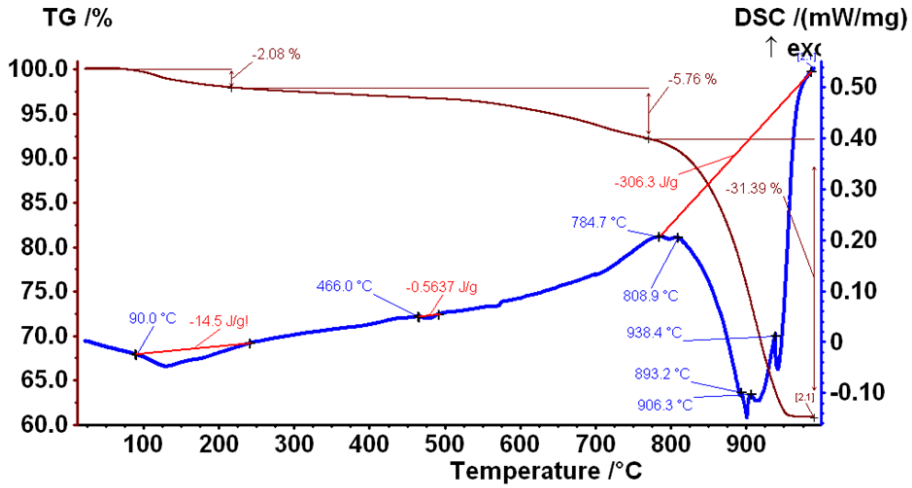

Figure 22: TGA results of IZ

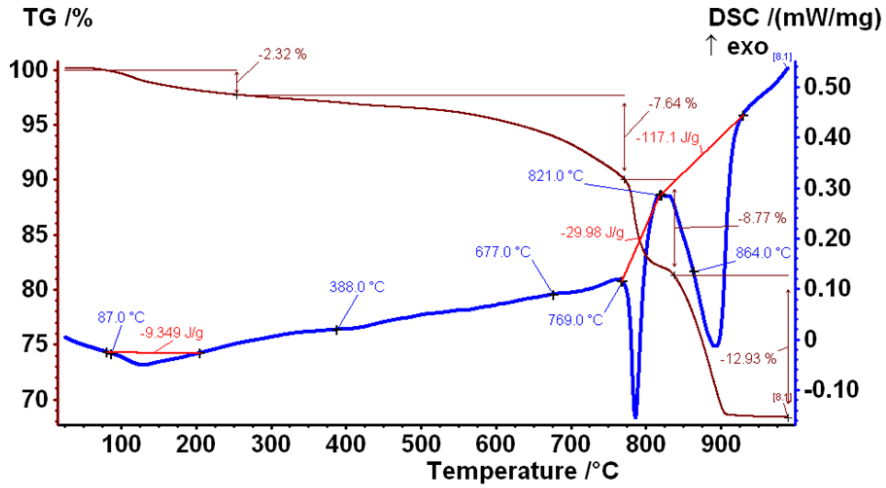

Figure 23: TGA results of MB

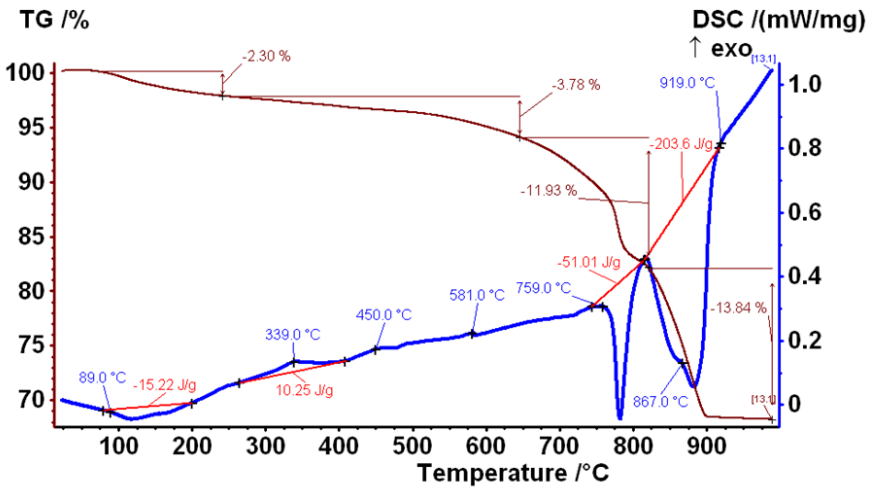

Figure 24: TGA results of NM

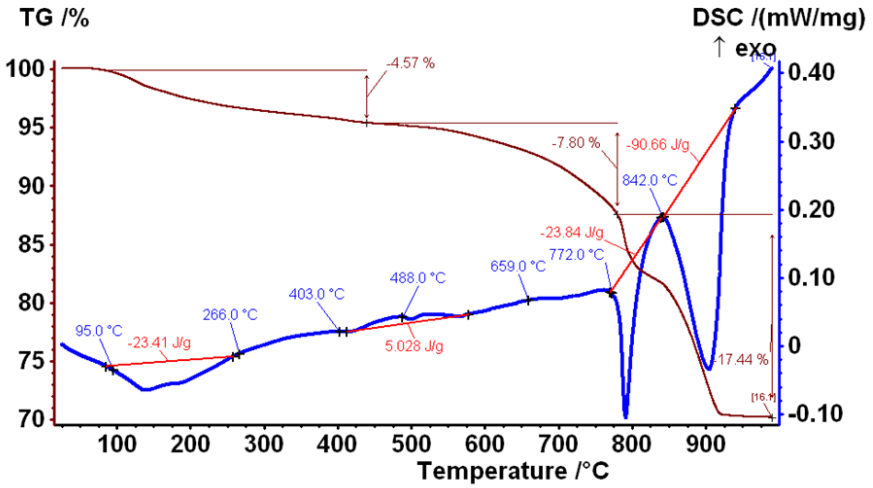

Figure 25: TGA results of SG

XRD analysis was performed to characterize the amorphous and crystalline mineral phases in the samples (Figure 26 to 30, Table 17 and 18). The used XRD device for construction debris was Philips Panalytical PW 3830/40 high voltage generator

(built in 2003) with a Philips model PW 2773/20 X-ray tube Cu anode and a Philips PW3710 diffractometer. The Cu X-ray light used had a wavelength of Kα1 = 1.54060 Å. An automatic aperture, a secondary graphite monochromator, and a proportional counter were utilized. Acquisition speed of imaging was 3.0° 2θ/minute (total 23 minutes), with an angular range from 2° to 70° 2θ (theta). The X'Pert HighScore 4.8 software was used for analyzing the data. For quantitative analysis the Rietveld analysis was performed.

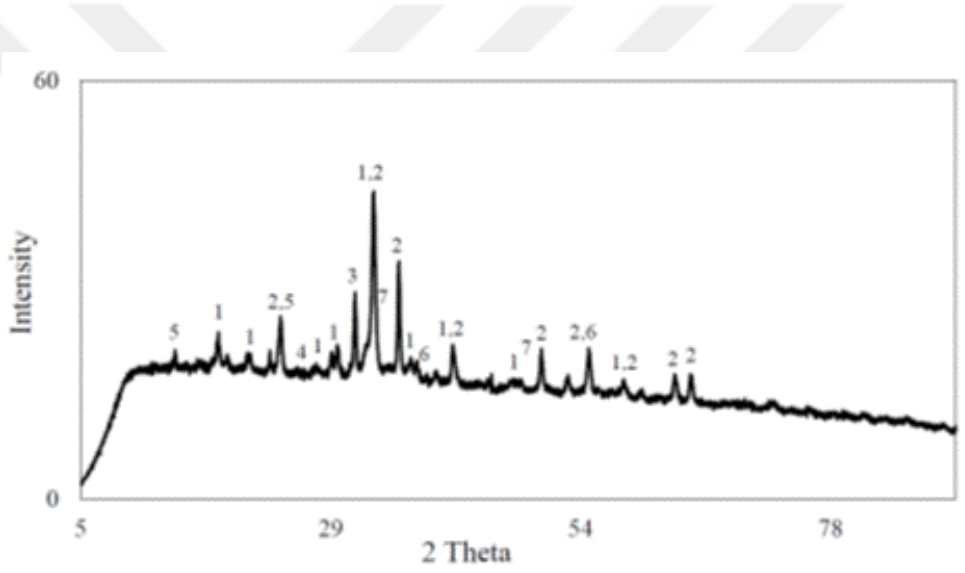

Figure 26: XRD results of RM after calcination

Table 17: Quantitative XRD results of RM

Peak number	*Phase name*	*Weight percent*	*Chemical formula*
1	Mayenite	34	$Ca_{12}Al_{14}O_{33}$
2	Hematite	41	Fe_2O_3
3	Dmisteinbergite	4	$CaAl_2Si_2O8$
4	Quartz	1	SiO_2
5	Cancrinite	8	$Na_6CaAl_6Si_6(CO_3)O_{24}.2H_2O$
6	Lime	5	CaO
7	Perovskite	7	$CaTiO_3$

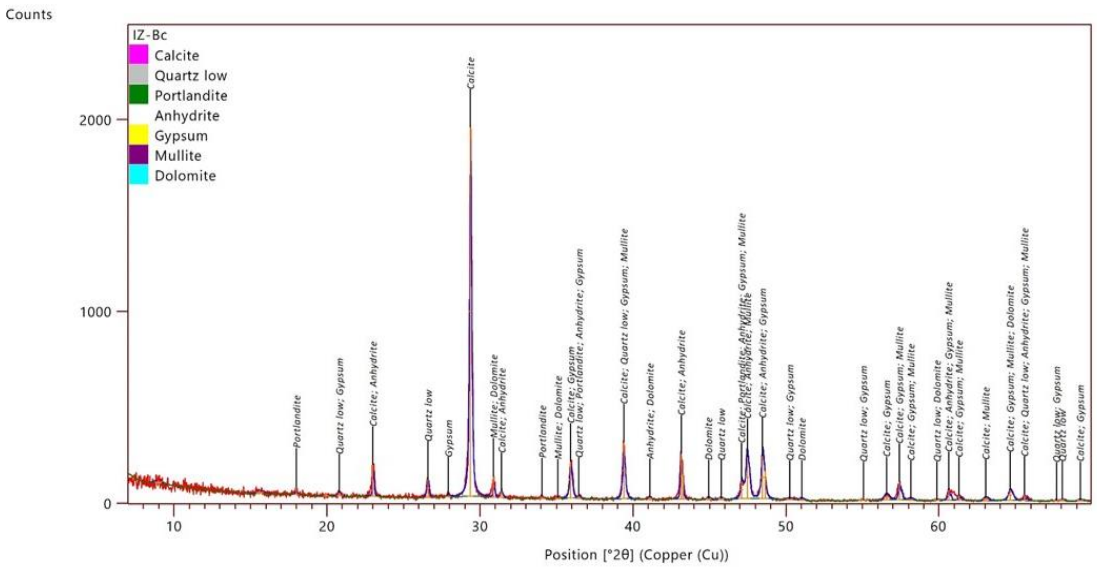

Figure 27: XRD results of IZ after calcination

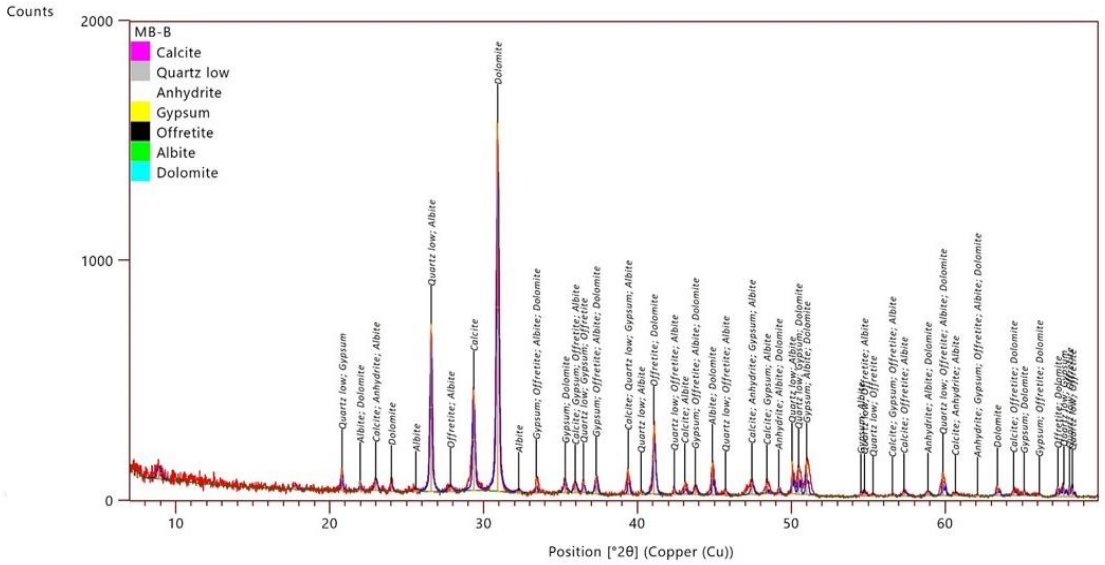

Figure 28: XRD results of MB after calcination

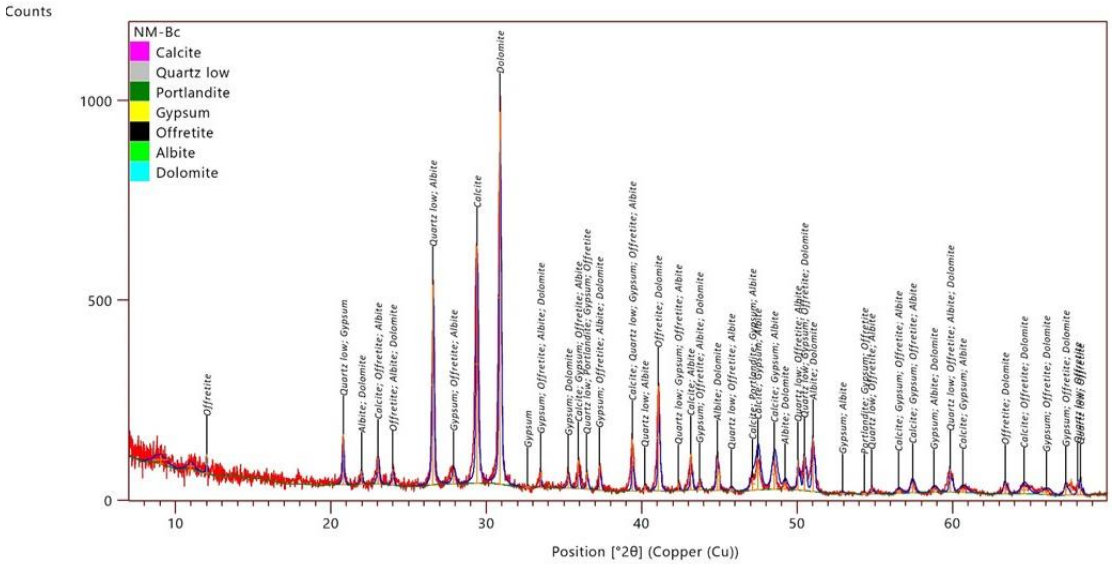

Figure 29: XRD results of NM after calcination

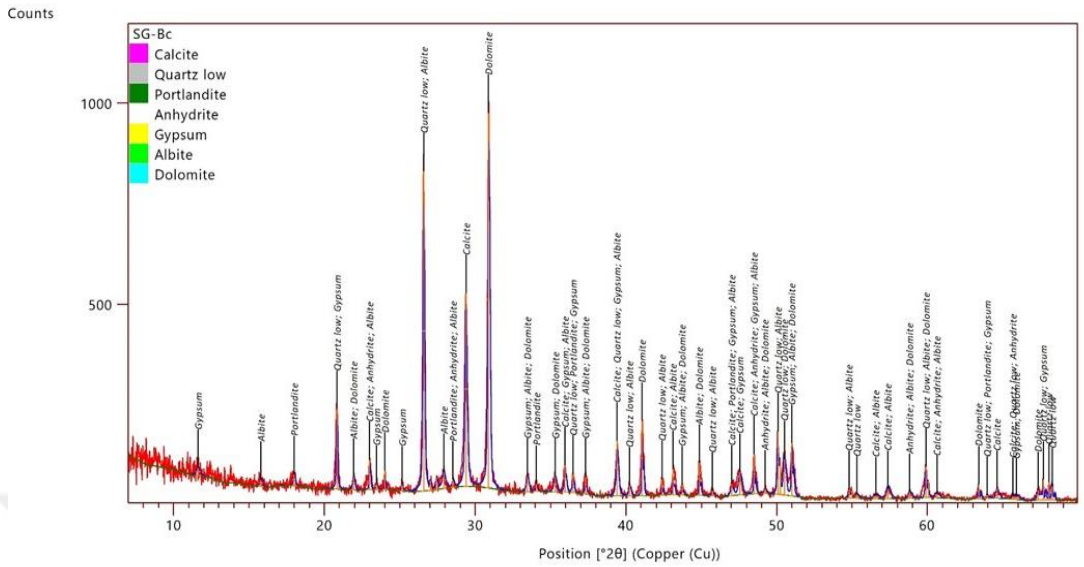

Figure 30: XRD results of SG after calcination

Table 18: Quantitative XRD results of IZ, MB, NM, and SG: Major phases, averaged

Peak number	*Phase name*	*Weight percent*	*Chemical formula*
1	Calcite	27.51	$CaCO_3$
2	Quartz	9.16	SiO_2
3	Dolomite	28.01	$MgCO_3.CaCO_3$
4	Amorphous	34.22	-
5	Other	1.10	-

The SEM test was also performed on RM samples (Figure 31). The plate like morphology of the materials can be observed from the results.

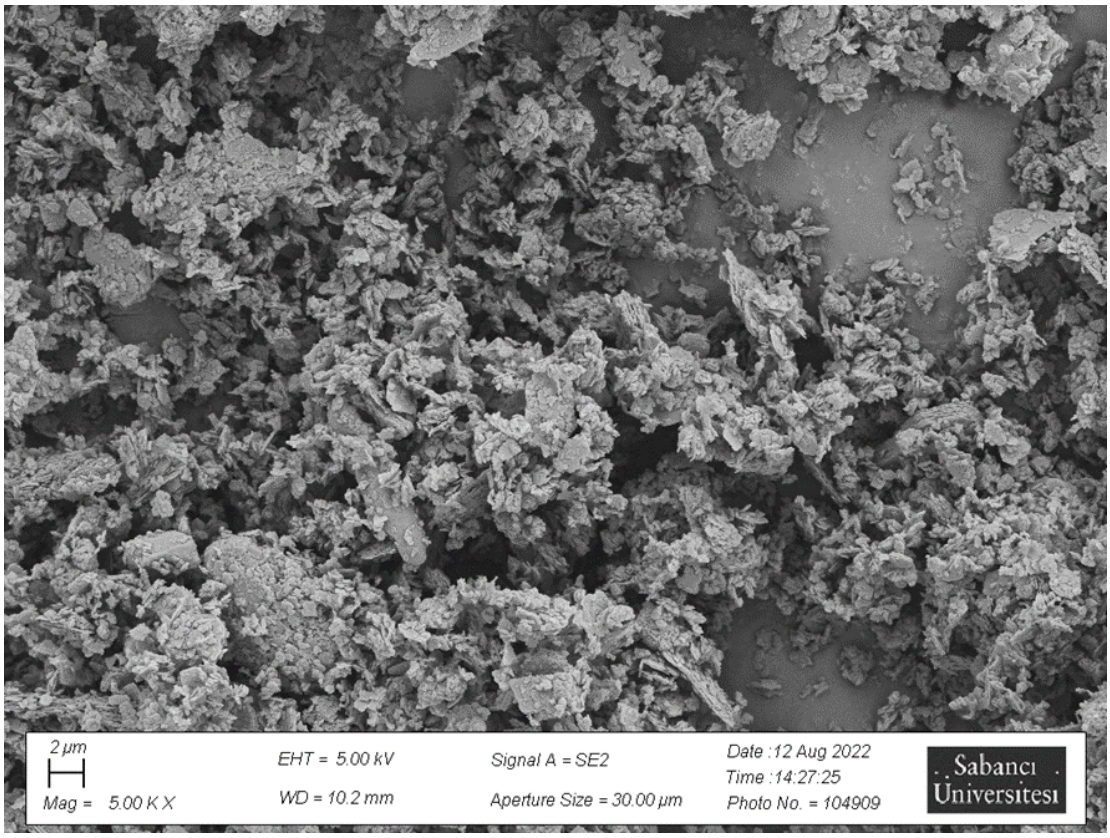

Figure 31: SEM result of RM

APPENDIX B:
Rheological curves

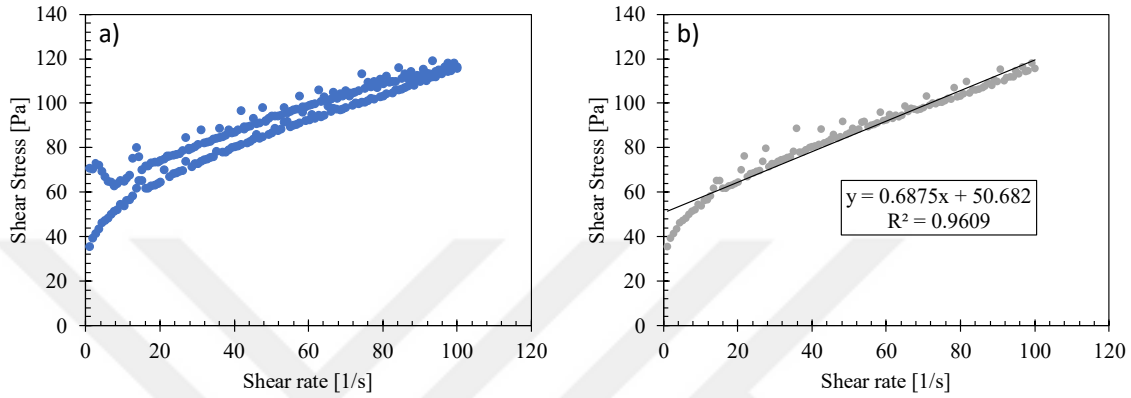

Figure 32: Rheological curve of Control_SP samples a) Full curve, and b) only down curve for regression

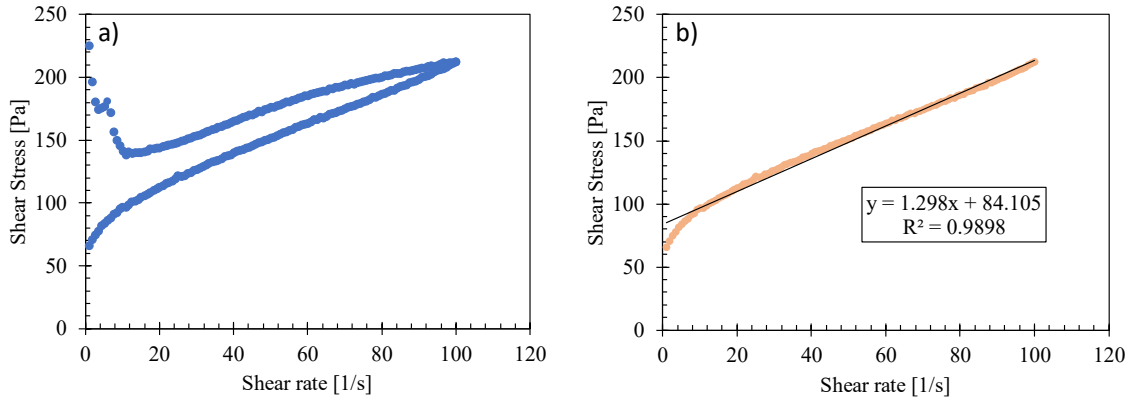

Figure 33: Rheological curve of RM_15 samples a) Full curve, and b) only down curve for regression

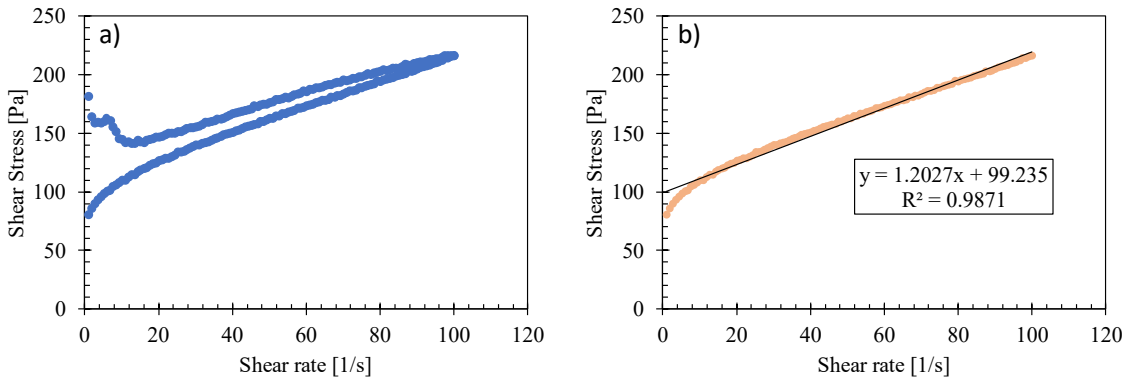

Figure 34: Rheological curve of RM_20 samples a) Full curve, and b) only down curve for regression

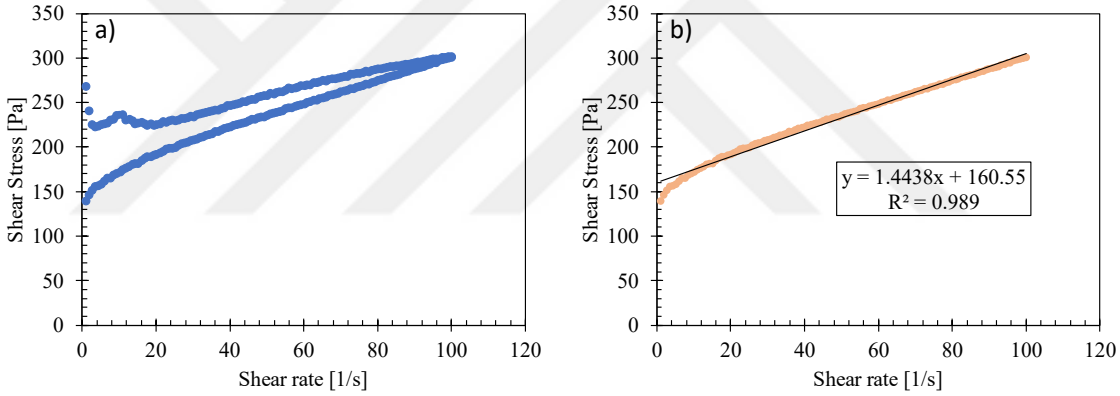

Figure 35: Rheological curve of RM_25 samples a) Full curve, and b) only down curve for regression

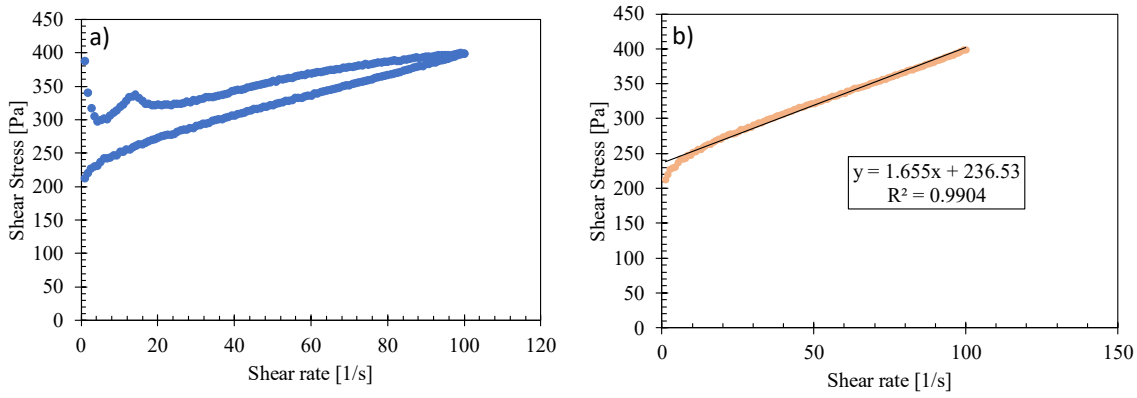

Figure 36: Rheological curve of RM_30 samples a) Full curve, and b) only down curve for regression

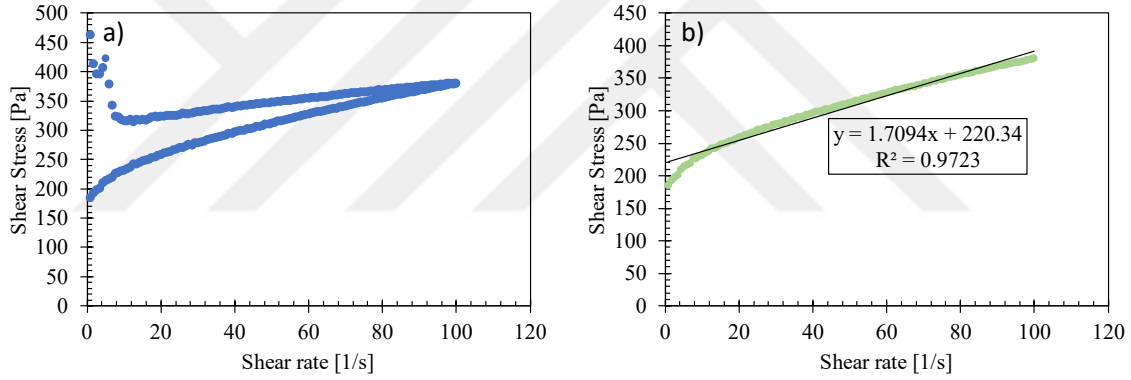

Figure 37: Rheological curve of MK_15 samples a) Full curve, and b) only down curve for regression

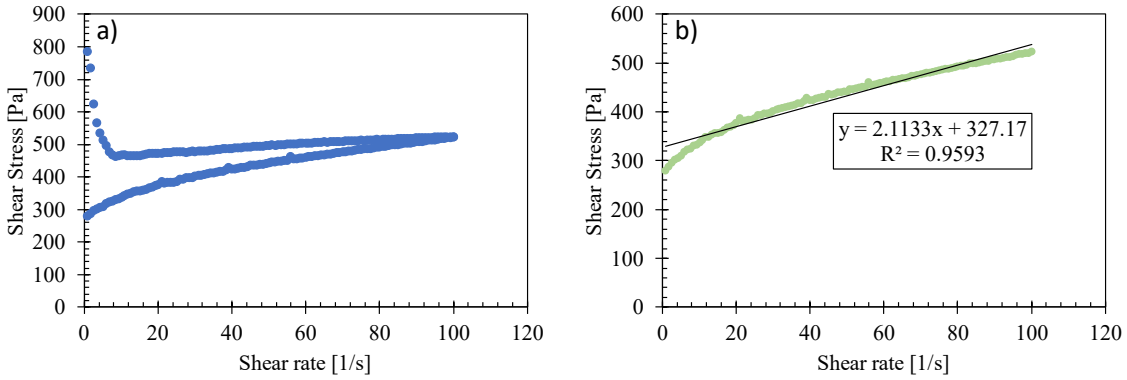

Figure 38: Rheological curve of MK_20 samples a) Full curve, and b) only down curve for regression

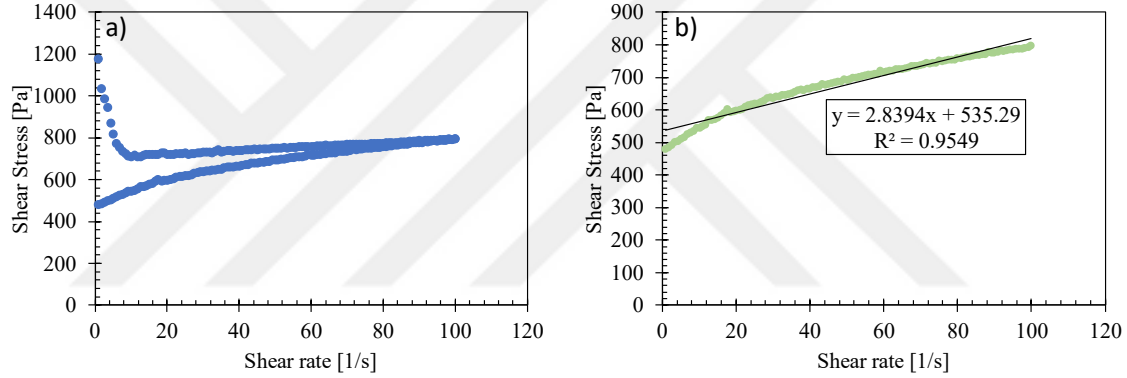

Figure 39: Rheological curve of MK_25 samples a) Full curve, and b) only down curve for regression

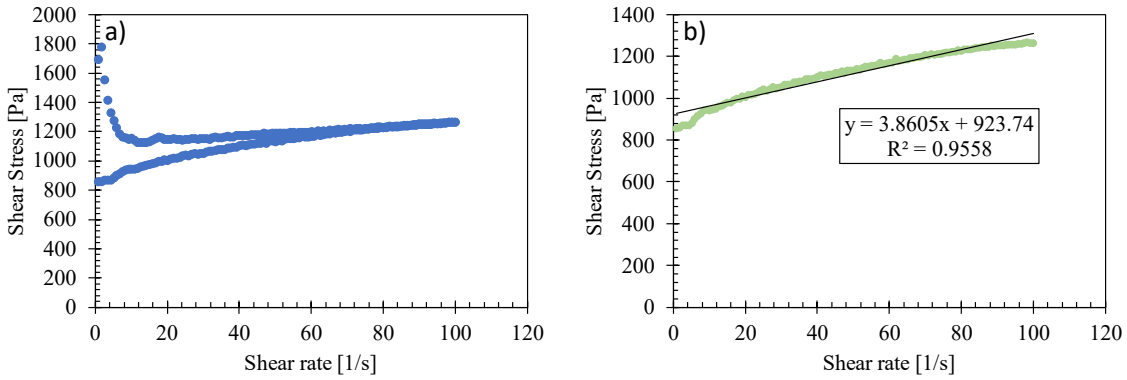

Figure 40: Rheological curve of MK_30 samples a) Full curve, and b) only down curve for regression

APPENDIX C:
The ANN code used in the study

The MATLAB code written for building the model is as follows:

```
filename='MK.xlsx';

x=xlsread(filename,'A1:C24');

y=xlsread(filename, 'D1:D24');
```

% In this section the excel file containing the compressive strength are read and columns are given certain names to be called. MK.xlsx is the file containing the results of MK. The code was repeated for all SCMs used in this study.

```
for i=1:3;

    x2(:,i)=(x(:,i)-min(x(:,i)))/(max(x(:,i))-min(x(:,i)));

end
```

% In this section the values of variables are normalized.

```
xt=x2';

yt=y';

hiddenLayerSize=7;

net=fitnet(hiddenLayerSize);

net.divideParam.trainRatio=87/100;
```

```
net.divideParam.valRatio=13/100;

net.divideParam.testRatio=0/100;

[net,tr]=train(net,xt,yt);
```

% In this section the model is trained. One hidden layer is chosen with 7 neurons in the final model. 87% of the data points were used as training data and the remaining 13 percent were used as validating data.

```
yTrain=net(xt(:,tr.trainInd));

yTrainTrue=yt(:,tr.trainInd);

sqrt(mean((yTrain-yTrainTrue).^2))

yVal=net(xt(:,tr.valInd));

yValTrue=yt(:,tr.valInd);

sqrt(mean((yVal-yValTrue).^2))

mdl=fitlm(yTrainTrue,yTrain)
```

% In this section the result of the model is compared with experimental results. The route mean square error (RMSE) was also calculated, as well as R^2 values.

```
for i=1:60

        hiddenLayerSize=i;

        net=fitnet(hiddenLayerSize);

        net.divideParam.trainRatio=92/100;

        net.divideParam.valRatio=8/100;
```

```
        net.divideParam.testRatio=0/100;

        [net,tr]=train(net,xt,yt);

        yTrain=net(xt(:,tr.trainInd));

        yTrainTrue=yt(:,tr.trainInd);

        yVal=net(xt(:,tr.valInd));

        yValTrue=yt(:,tr.valInd);

        rmse_train(i)=sqrt(mean((yTrain-yTrainTrue).^2))

        rmse_val(i)=sqrt(mean((yVal-yValTrue).^2))

    end

    plot(1:60,rmse_train); hold on;

    plot(1:60,rmse_val); hold off;
```

% In this section, a loop is run for finding the optimum number of neurons to be used in the hidden layer. The number of neurons corresponding to the lowest RMSE values for both training and validating data was chosen. The RMSE for all cases was kept under 2 MPa.

REFERENCES

[1] K. L. Scrivener and A. Nonat, “Hydration of cementitious materials, present and future,” *Cement and Concrete Research*, vol. 41, no. 7. 2011. doi: 10.1016/j.cemconres.2011.03.026.

[2] R. Jaskulski, D. Jóźwiak-Niedźwiedzka, and Y. Yakymechko, “Calcined clay as supplementary cementitious material,” *Materials*, vol. 13, no. 21. 2020. doi: 10.3390/ma13214734.

[3] N. Zhang *et al.*, “On the incorporation of class F fly-ash to enhance the geopolymerization effects and splitting tensile strength of the gold mine tailings-based geopolymer,” *Constr. Build. Mater.*, vol. 308, 2021, doi: 10.1016/j.conbuildmat.2021.125112.

[4] S. Dadsetan, H. Siad, M. Lachemi, and M. Sahmaran, “Construction and demolition waste in geopolymer concrete technology: A review,” *Magazine of Concrete Research*, vol. 71, no. 23. 2019. doi: 10.1680/jmacr.18.00307.

[5] S. Moukannaa, A. Nazari, A. Bagheri, M. Loutou, J. G. Sanjayan, and R. Hakkou, “Alkaline fused phosphate mine tailings for geopolymer mortar synthesis: Thermal stability, mechanical and microstructural properties,” *J. Non. Cryst. Solids*, vol. 511, 2019, doi: 10.1016/j.jnoncrysol.2018.12.031.

[6] N. Zhang, B. Tang, and X. Liu, “Cementitious activity of iron ore tailing and its utilization in cementitious materials, bricks and concrete,” *Constr. Build. Mater.*, vol. 288, 2021, doi: 10.1016/j.conbuildmat.2021.123022.

[7] X. He *et al.*, “Mine tailings-based geopolymers: A comprehensive review,” *Ceram. Int.*, vol. 48, no. 17, pp. 24192–24212, 2022, doi: 10.1016/j.ceramint.2022.05.345.

[8] C. R. Gagg, “Cement and concrete as an engineering material: An historic appraisal and case study analysis,” *Eng. Fail. Anal.*, vol. 40, 2014, doi: 10.1016/j.engfailanal.2014.02.004.

[9] Y. Chen, S. C. Figueiredo, Ç. Yalçinkaya, O. Çopuroğlu, F. Veer, and E. Schlangen, “The effect of viscosity-modifying admixture on the extrudability of limestone and calcined clay-based cementitious material for extrusion-based 3D concrete printing,” *Materials (Basel).*, vol. 12, no. 9, 2019, doi: 10.3390/ma12091374.

[10] S. A. Khedr and M. N. Abou-Zeid, “Characteristics of Silica-Fume Concrete,” *J. Mater. Civ. Eng.*, vol. 6, no. 3, 1994, doi: 10.1061/(asce)0899-1561(1994)6:3(357).

[11] K. Murari, R. Siddique, and K. K. Jain, “Use of waste copper slag, a sustainable material,” *Journal of Material Cycles and Waste Management*, vol. 17, no. 1. 2015. doi: 10.1007/s10163-014-0254-x.

[12] Juan Rodriguez, “Uses, benefits and drawbacks of fly ash in construction,”

Dotdash , 2021.

[13] K. Scrivener and A. Favier, *Calcined Clays for Sustainable Concrete*. 2015. doi: 10.1007/978-94-017-9939-3.

[14] B. Sabir, S. Wild, and J. Bai, "Metakaolin and calcined clays as pozzolans for concrete: A review," *Cem. Concr. Compos.*, vol. 23, no. 6, 2001, doi: 10.1016/S0958-9465(00)00092-5.

[15] S. Wild and J. M. Khatib, "Portlandite consumption in metakaolin cement pastes and mortars," *Cem. Concr. Res.*, vol. 27, no. 1, 1997, doi: 10.1016/S0008-8846(96)00187-1.

[16] B. Ahmadi and M. Shekarchi, "Use of natural zeolite as a supplementary cementitious material," *Cem. Concr. Compos.*, vol. 32, no. 2, 2010, doi: 10.1016/j.cemconcomp.2009.10.006.

[17] S. C. Taylor-Lange, E. L. Lamon, K. A. Riding, and M. C. G. Juenger, "Calcined kaolinite-bentonite clay blends as supplementary cementitious materials," *Appl. Clay Sci.*, vol. 108, 2015, doi: 10.1016/j.clay.2015.01.025.

[18] C. R. Wu, Z. Q. Hong, B. J. Zhan, W. Tang, S. C. Cui, and S. C. Kou, "Effect of acid treatment on the reactivity of natural sepiolite used as a supplementary cementitious material," *Constr. Build. Mater.*, vol. 316, 2022, doi: 10.1016/j.conbuildmat.2021.125860.

[19] R. Fernandez, F. Martirena, and K. L. Scrivener, "The origin of the pozzolanic activity of calcined clay minerals: A comparison between kaolinite, illite and montmorillonite," *Cem. Concr. Res.*, vol. 41, no. 1, 2011, doi: 10.1016/j.cemconres.2010.09.013.

[20] E. Aprianti, P. Shafigh, S. Bahri, and J. N. Farahani, "Supplementary cementitious materials origin from agricultural wastes - A review," *Construction and Building Materials*, vol. 74. 2015. doi: 10.1016/j.conbuildmat.2014.10.010.

[21] M. C. Bignozzi and A. Saccani, "Ceramic waste as aggregate and supplementary cementing material: A combined action to contrast alkali silica reaction (ASR)," *Cem. Concr. Compos.*, vol. 34, no. 10, 2012, doi: 10.1016/j.cemconcomp.2012.07.001.

[22] M. Mirzahosseini and K. A. Riding, "Influence of different particle sizes on reactivity of finely ground glass as supplementary cementitious material (SCM)," *Cem. Concr. Compos.*, vol. 56, 2015, doi: 10.1016/j.cemconcomp.2014.10.004.

[23] *The Concrete Centre, Mineral Products Association*, 2019th ed. 2019.

[24] *European Commission (DG ENV) Service Contract on Management of Construction And Demolition Waste 2, SR1 Final Report Task*.

[25] A. A. Aliabdo, A. E. M. Abd Elmoaty, and E. M. Auda, "Re-use of waste marble dust in the production of cement and concrete," *Constr. Build. Mater.*, vol. 50, 2014, doi: 10.1016/j.conbuildmat.2013.09.005.

[26] G. Ma, Z. Li, and L. Wang, "Printable properties of cementitious material

containing copper tailings for extrusion based 3D printing," *Constr. Build. Mater.*, vol. 162, 2018, doi: 10.1016/j.conbuildmat.2017.12.051.

[27] M. Juenger *et al.*, "Supplementary cementitious materials for concrete: Characterization needs," in *Materials Research Society Symposium Proceedings*, 2012, vol. 1488. doi: 10.1557/opl.2012.1536.

[28] H. F. W. Taylor, "Cement chemistry. 2nd ed.," *Acad. Press*, vol. 20, no. 4, 1997.

[29] British Standard Institution, "EN 196-1: 2016 Methods of Testing Cement - Part 1: Determination of Strength," *Br. Stand.*, 2016.

[30] American Society for Testing and Materials, "ASTM C305-14 - Standard Practice for Mechanical Mixing of Hydraulic Cement Pastes and Mortars of Plastic Consistency," *ASTM Int.*, vol. 04, no. 01, p. 3, 2009.

[31] ASTM C1437, "Standard Test Method for Flow of Hydraulic Cement Mortar: C1437-15," *Standard*, 2015.

[32] M. K. Rahman, M. H. Baluch, and M. A. Malik, "Thixotropic behavior of self compacting concrete with different mineral admixtures," *Constr. Build. Mater.*, vol. 50, 2014, doi: 10.1016/j.conbuildmat.2013.10.025.

[33] ASTM C109, "ASTM C109 / C109M - 20b. Standard Test Method for Compressive Strength of Hydraulic Cement Mortars (Using 2-in. or [50 mm] Cube Specimens)," *Annual Book of ASTM Standards*, vol. 04. 2020.

[34] L. Chen, "A multiple linear regression prediction of concrete compressive strength based on physical properties of electric arc furnace oxidizing slag," *Iternational Journal of Applied Science and Engineering*, vol. 7,2. 2010.

[35] "Commission 25-PEM Protection et érosion des monuments," *Matériaux Constr.*, vol. 13, no. 3, 1980, doi: 10.1007/bf02473564.

[36] ASTM Committee C01.29, "ASTM C1012/C1012M –15: Standard Test Method for Length Change of Hydraulic-Cement Mortars Exposed to a Sulfate Solution," in *Annual Book of ASTM Standards Volume 04.01*, 2015.

[37] ASTM I, "ASTM C1567-1314 - Standard Test Method for Determining the Potential Alkali-Silica Reactivity of Combinations of Cementitious Materials and Aggregate (Accelerated Mortar-Bar Method)," *ASTM Int.*, 2013.

[38] *NF P18-513: Metakaolin. Pozzolanic addition for concrete. Definitions, specifications and conformity criteria*. La Plaine Saint-Denis: Association Française de Normalisation, 2010.

[39] C. Kuenzel, L. J. Vandeperre, S. Donatello, A. R. Boccaccini, and C. Cheeseman, "Ambient temperature drying shrinkage and cracking in metakaolin-based geopolymers," *J. Am. Ceram. Soc.*, vol. 95, no. 10, 2012, doi: 10.1111/j.1551-2916.2012.05380.x.

[40] A. U. Elinwa, "Experimental characterization of Portland cement-calcined soldier-ant mound clay cement mortar and concrete," *Constr. Build. Mater.*, vol. 20, no. 9, 2006, doi: 10.1016/j.conbuildmat.2005.01.053.

[41] N. Salem, M. Ltifi, and H. Hassis, “Mechanical and durability study of Tunisian calcined clay in lightweight concrete of expanded clay,” *Eur. J. Environ. Civ. Eng.*, vol. 25, no. 12, 2021, doi: 10.1080/19648189.2019.1624625.

[42] M. A. Caldarone, K. A. Gruber, and R. G. Burg, “High-reactivity metakaolin: a new generation mineral admixture,” *Concr. Int.*, vol. 16, no. 11, 1994.

[43] M. Lorena Figueiredo Martins, P. Roberto Ribeiro Soares Junior, T. Henrique da Silva, P. de Souza Maciel, I. Peixoto Pinheiro, and A. Cesar da Silva Bezerra, “Magnesium industry waste and red mud to eco-friendly ternary binder: Producing more sustainable cementitious materials,” *Constr. Build. Mater.*, vol. 310, 2021, doi: 10.1016/j.conbuildmat.2021.125172.

[44] S. Rols, M. Mbessa, J. Ambroise, and J. Pera, “Influence of ultra-fine particle type on properties of very-high-strength concrete,” in *American Concrete Institute, ACI Special Publication*, 1999, vol. SP186. doi: 10.14359/5584.

[45] K. A. Melo and A. M. P. Carneiro, “Effect of Metakaolin’s finesses and content in self-consolidating concrete,” *Constr. Build. Mater.*, vol. 24, no. 8, 2010, doi: 10.1016/j.conbuildmat.2010.02.002.

[46] X. Chen, Y. Li, Z. Zhu, and L. Ma, “Evaluation of waste concrete recycled powder (WCRP) on the preparation of low-exothermic cement,” *J. Build. Eng.*, vol. 53, no. April, 2022, doi: 10.1016/j.jobe.2022.104511.

[47] X. F. Chen and C. J. Jiao, “Effect of construction wastes on the rheo-physical behavior of photocatalytic mortar,” *Case Stud. Constr. Mater.*, vol. 16, no. March, 2022, doi: 10.1016/j.cscm.2022.e01049.

[48] I. Janotka, F. Puertas, M. Palacios, M. Kuliffayová, and C. Varga, “Metakaolin sand-blended-cement pastes: Rheology, hydration process and mechanical properties,” *Constr. Build. Mater.*, vol. 24, no. 5, 2010, doi: 10.1016/j.conbuildmat.2009.10.028.

[49] Y. Chen, C. Romero Rodriguez, Z. Li, B. Chen, O. Çopuroğlu, and E. Schlangen, “Effect of different grade levels of calcined clays on fresh and hardened properties of ternary-blended cementitious materials for 3D printing,” *Cem. Concr. Compos.*, vol. 114, 2020, doi: 10.1016/j.cemconcomp.2020.103708.

[50] J. Assaad and K. H. Khayat, “Assessment of Thixotropy of Self-Consolidating Concrete and Concrete-Equivalent-Mortar - Effect of Binder Composition and Content,” *ACI Mater. J.*, vol. 101, no. 5, 2004, doi: 10.14359/13426.

[51] S. Ng and J. Plank, “Interaction mechanisms between Na montmorillonite clay and MPEG-based polycarboxylate superplasticizers,” *Cem. Concr. Res.*, vol. 42, no. 6, 2012, doi: 10.1016/j.cemconres.2012.03.005.

[52] and K. W. H. A. Barnes, J. F. Hutton, “An Introduction to Rheology,” 3rd editio., Elsevier Science, 1989.

[53] B. Panda, N. A. N. Mohamed, S. C. Paul, G. V. P. B. Singh, M. J. Tan, and B. Šavija, “The effect of material fresh properties and process parameters on buildability and interlayer adhesion of 3D printed concrete,” *Materials (Basel).*, vol. 12, no. 13, 2019, doi: 10.3390/ma12132149.

[54] ASSOCIAÇÃO BRASILEIRA DE NORMAS TÉCNICAS., “ABNT NBR 5752- Materiais pozolânicos — Determinação do índice de desempenho com cimento Portland aos 28 dias,” *Assoc. Bras. Normas Técnicas*, 2014.

[55] ASTM C618-17a, “Standard specification for coal fly ash and raw or calcined natural pozzolan for use in concrete,” *Annu. B. ASTM Stand.*, 2017.

[56] Y. Wang, X. Liu, Z. Xie, H. Wang, W. Zhang, and Y. Xue, “Rapid evaluation of the pozzolanic activity of bayer red mud by a polymerization degree method: Correlations with alkali dissolution of (si+al) and strength,” *Materials (Basel).*, vol. 14, no. 19, 2021, doi: 10.3390/ma14195546.

[57] C. Venkatesh, N. Ruben, and M. S. R. Chand, “Red mud as an additive in concrete: comprehensive characterization,” *J. Korean Ceram. Soc.*, vol. 57, no. 3, 2020, doi: 10.1007/s43207-020-00030-3.

[58] M. Zhou, P. Chen, X. Chen, X. Ge, and Y. Wang, “Study on hydration characteristics of circulating fluidized bed combustion fly ash (CFBCA),” *Constr. Build. Mater.*, vol. 251, 2020, doi: 10.1016/j.conbuildmat.2020.118993.

[59] Y. Wang *et al.*, “Effects of Si/Al ratio on the efflorescence and properties of fly ash based geopolymer,” *J. Clean. Prod.*, vol. 244, 2020, doi: 10.1016/j.jclepro.2019.118852.

[60] G. Gelardi and R. J. Flatt, “Working mechanisms of water reducers and superplasticizers,” in *Science and Technology of Concrete Admixtures*, 2016. doi: 10.1016/B978-0-08-100693-1.00011-4.

[61] J. H. Ideker, K. L. Scrivener, H. Fryda, and B. Touzo, “Calcium aluminate cements,” in *Lea’s Chemistry of Cement and Concrete*, 2019. doi: 10.1016/B978-0-08-100773-0.00012-5.

[62] S. Wild, J. M. Khatib, and A. Jones, “Relative strength, pozzolanic activity and cement hydration in superplasticised metakaolin concrete,” *Cem. Concr. Res.*, vol. 26, no. 10, 1996, doi: 10.1016/0008-8846(96)00148-2.

[63] F. Curcio, B. A. DeAngelis, and S. Pagliolico, “Metakaolin as a pozzolanic microfiller for high-performance mortars,” *Cem. Concr. Res.*, vol. 28, no. 6, 1998, doi: 10.1016/S0008-8846(98)00045-3.

[64] Y. Chen *et al.*, “Effect of printing parameters on interlayer bond strength of 3D printed limestone-calcined clay-based cementitious materials: An experimental and numerical study,” *Constr. Build. Mater.*, vol. 262, 2020, doi: 10.1016/j.conbuildmat.2020.120094.

[65] F. Avet, R. Snellings, A. Alujas Diaz, M. Ben Haha, and K. Scrivener, “Development of a new rapid, relevant and reliable (R3) test method to evaluate the pozzolanic reactivity of calcined kaolinitic clays,” *Cem. Concr. Res.*, vol. 85, 2016, doi: 10.1016/j.cemconres.2016.02.015.

[66] F. Avet and K. Scrivener, “Investigation of the calcined kaolinite content on the hydration of Limestone Calcined Clay Cement (LC3),” *Cem. Concr. Res.*, vol. 107, 2018, doi: 10.1016/j.cemconres.2018.02.016.

[67] Y. Chen, Z. Li, S. C. Figueiredo, O. Çopuroğlu, F. Veer, and E. Schlangen, "Limestone and Calcined Clay-Based Sustainable Cementitious Materials for 3D Concrete Printing: A Fundamental Study of Extrudability and Early-Age Strength Development," *Appl. Sci.*, vol. 9, no. 9, 2019, doi: 10.3390/app9091809.

[68] B. Lu *et al.*, "A systematical review of 3D printable cementitious materials," *Construction and Building Materials*, vol. 207. 2019. doi: 10.1016/j.conbuildmat.2019.02.144.

[69] D. Yang, M. Liu, Z. Zhang, P. Yao, and Z. Ma, "Properties and modification of sustainable foam concrete including eco-friendly recycled powder from concrete waste," *Case Stud. Constr. Mater.*, vol. 16, no. October 2021, 2022, doi: 10.1016/j.cscm.2021.e00826.

[70] M. C. G. Juenger, F. Winnefeld, J. L. Provis, and J. H. Ideker, "Advances in alternative cementitious binders," *Cement and Concrete Research*, vol. 41, no. 12. 2011. doi: 10.1016/j.cemconres.2010.11.012.

[71] Z. E. A. Laidani, B. Benabed, R. Abousnina, M. K. Gueddouda, and M. J. Khatib, "Potential pozzolanicity of Algerian calcined bentonite used as cement replacement: optimisation of calcination temperature and effect on strength of self-compacting mortars," *Eur. J. Environ. Civ. Eng.*, vol. 26, no. 4, 2022, doi: 10.1080/19648189.2020.1713898.

[72] M. Ghalehnovi, N. Roshan, A. Taghizadeh, E. Asadi Shamsabadi, S. Ali Hadigheh, and J. de Brito, "Production of Environmentally Friendly Concrete Incorporating Bauxite Residue and Silica Fume," *J. Mater. Civ. Eng.*, vol. 34, no. 2, 2022, doi: 10.1061/(asce)mt.1943-5533.0004060.

[73] I. Vladić Kancir and M. Serdar, "Contribution to Understanding of Synergy between Red Mud and Common Supplementary Cementitious Materials," *Materials (Basel).*, vol. 15, no. 5, 2022, doi: 10.3390/ma15051968.

[74] J. Bizzozero, "Hydration and dimensional stability of calcium aluminate cement based systems," vol. 6336, 2014.

[75] Q. Tang, Z. Ma, H. Wu, and W. Wang, "The utilization of eco-friendly recycled powder from concrete and brick waste in new concrete: A critical review," *Cem. Concr. Compos.*, vol. 114, 2020, doi: 10.1016/j.cemconcomp.2020.103807.

[76] A. A. Hilal, N. H. Thom, and A. R. Dawson, "Pore structure and permeation characteristics of foamed concrete," *J. Adv. Concr. Technol.*, vol. 12, no. 12, 2014, doi: 10.3151/jact.12.535.

[77] *GB/T 2847-2005, pozzolanic Materials Used for Cement Production*. China: Standardization Administration of China, 2005.

[78] ASTM Committee C01.10, "ASTM C1157-11 Standard Performance Specification for Hydraulic Cement," in *Annual Book of ASTM Standards Volume 04.01*, 2011.

[79] BS-EN197-1:, "Cement Part 1: Composition, Specifications and Conformity Criteria for Common Cements," *Br. Stand.*, no. November, 2011.

[80] J. Castro, D. Bentz, and J. Weiss, “Effect of sample conditioning on the water absorption of concrete,” *Cem. Concr. Compos.*, vol. 33, no. 8, 2011, doi: 10.1016/j.cemconcomp.2011.05.007.

[81] S. Kelham, “A water absorption test for concrete,” *Mag. Concr. Res.*, vol. 40, no. 143, 1988, doi: 10.1680/macr.1988.40.143.106.

[82] L. Courard, A. Darimont, M. Schouterden, F. Ferauche, X. Willem, and R. Degeimbre, “Durability of mortars modified with metakaolin,” *Cem. Concr. Res.*, vol. 33, no. 9, 2003, doi: 10.1016/S0008-8846(03)00090-5.

[83] M. Ghalehnovi, N. Roshan, E. Hakak, E. A. Shamsabadi, and J. de Brito, “Effect of red mud (bauxite residue) as cement replacement on the properties of self-compacting concrete incorporating various fillers,” *J. Clean. Prod.*, vol. 240, 2019, doi: 10.1016/j.jclepro.2019.118213.

[84] I. M. Nikbin, M. Aliaghazadeh, Sh Charkhtab, and A. Fathollahpour, “Environmental impacts and mechanical properties of lightweight concrete containing bauxite residue (red mud),” *J. Clean. Prod.*, vol. 172, 2016, doi: 10.1016/j.jclepro.2017.11.143.

[85] M. A. Haque, B. Chen, and Y. Liu, “The role of bauxite and fly-ash on the water stability and microstructural densification of magnesium phosphate cement composites,” *Constr. Build. Mater.*, vol. 260, 2020, doi: 10.1016/j.conbuildmat.2020.119953.

[86] S. Li, J. Gao, Q. Li, and X. Zhao, “Investigation of using recycled powder from the preparation of recycled aggregate as a supplementary cementitious material,” *Constr. Build. Mater.*, vol. 267, 2021, doi: 10.1016/j.conbuildmat.2020.120976.

[87] A. Rossetti, T. Ikumi, I. Segura, and E. F. Irassar, “Sulfate Resistance of Blended Cements (Limestone Illite Calcined Clay) Exposed Without Previous Curing,” *Curr. Top. Trends Durab. Build. Mater. Components - Proc. 15th Int. Conf. Durab. Build. Mater. Components, DBMC 2020*, pp. 1625–1632, 2020, doi: 10.23967/dbmc.2020.224.

[88] N. M. Al-Akhras, “Durability of metakaolin concrete to sulfate attack,” *Cem. Concr. Res.*, vol. 36, no. 9, 2006, doi: 10.1016/j.cemconres.2006.03.026.

[89] C. H. Aramburo, C. Pedrajas, and R. Talero, “Portland cements with high content of calcined clay: Mechanical strength behaviour and sulfate durability,” *Materials (Basel).*, vol. 13, no. 18, 2020, doi: 10.3390/MA13184206.

[90] K. Mehta and P. J. M. Monteiro, *Concrete: Microstructure, Properties, and Materials*. McGraw-Hill Education.

[91] J. A. Kostuch, V. Walters, and T. R. Jones, “High performance concretes incorporating metakaolin: a review,” *IConcrete 2000 Econ. durable Constr. through Excell. Proc. Int. Conf. Vol 2; Infrastructure, Res. new Appl.*, vol. 2, pp. 1799–1812, 1993.

[92] J. Sarfo-Ansah, E. Atiemo, K. A. Boakye, D. Adjei, and A. A. Adjaottor, “Calcined Clay Pozzolan as an Admixture to Mitigate the Alkali-Silica Reaction in Concrete,” *J. Mater. Sci. Chem. Eng.*, vol. 02, no. 05, 2014, doi:

10.4236/msce.2014.25004.

[93] L. Senff, R. C. E. Modolo, A. S. Silva, V. M. Ferreira, D. Hotza, and J. A. Labrincha, “Influence of red mud addition on rheological behavior and hardened properties of mortars,” *Constr. Build. Mater.*, vol. 65, 2014, doi: 10.1016/j.conbuildmat.2014.04.104.

VITA

EDUCATION

Master of Science student in Civil Engineering department at **Özyeğin University**. *February 2021-Present.* Thesis title: "Experimental And Analytical Study On The Performance Of Cementitious Mixes Containing different Re-generated End Of Life Materials"

Bachelor of Engineering Science, Civil Engineering at **Sharif University of Technology**, *September 2016-September 2020.*

ACADEMIC EMPLOYMENT

Graduate Teaching Assistant, department of Civil Engineering, Özyeğin University, *February 2021-Present.*

PUBLICATION

Mahmoudi, Matineh., Basaran Bundur, Zeynep., Yılmaz, Taner. "Use of analytical methods for estimating performance of concrete and their implementation to 3D printing: A systematic review".